Applied Catalysis B: Environmental 199 (2016) 199–223

Contents lists available at ScienceDirect

Applied Catalysis B: Environmental

journal homepage: www.elsevier.com/locate/apcatb

Review

Solar disinfection is an augmentable, *in situ*-generated photo-Fenton reaction—Part 1: A review of the mechanisms and the fundamental aspects of the process

Stefanos Giannakis[a], María Inmaculada Polo López[b,c], Dorothee Spuhler[a], Jose Antonio Sánchez Pérez[c], Pilar Fernández Ibáñez[b,c,**], César Pulgarin[a,*]

[a] SB, ISIC, Group of Advanced Oxidation Processes, Ecole Polytechnique Fédérale de Lausanne (EPFL), Station 6, 1015 Lausanne, Switzerland
[b] Plataforma Solar de Almería – CIEMAT, P.O. Box 22, Tabernas, Almería 04200, Spain
[c] CIESOL, Joint Centre of the University of Almería-CIEMAT, 04120 Almería, Spain

ARTICLE INFO

Article history:
Received 1 April 2016
Received in revised form 28 May 2016
Accepted 2 June 2016
Available online 8 June 2016

Keywords:
Solar disinfection
Near-neutral photo-Fenton
Light-bacteria interaction
Photocatalytic mechanisms
Photo-chemistry
Photo-biology

ABSTRACT

The present manuscript is a conceptual review concerning the photo-Fenton reaction at near-neutral pH, used for bacterial inactivation. In this first Part, an overview of the mechanisms involved, as well as the fundamental concepts governing the near-neutral photo-Fenton reaction are critically assessed. The two constituents of the process, namely solar light and the Fenton reagents, are dissociated, with their direct and indirect actions thoroughly analyzed. The effects of UVB and UVA on the bacterial cell are firstly discussed, followed by the presentation of the indirect oxidative stress-related inactivation mechanisms initiated into the microorganism, in presence of light. Afterwards, the effect of each Fenton reagent (H_2O_2, Fe) is analyzed in a step-wise manner, with H_2O_2 and Fe as enhancements of the solar disinfection mode of action. This approach proves that in fact, the solar photo-Fenton reaction is an enhanced solar disinfection process. Finally, the photo-Fenton reaction is put into context by considering the possible interactions of the separate parts of the combined process with the constituents of the natural environment that can play an important role in the evolution of the bacterial inactivation.

Contents

Abbreviations: AOP, advanced oxidation process; ATP, adenosine triphosphate; CAT, catalase; CDOM, chromoforic dissolved organic matter; CPC, compound parabolic collector; CPD, cyclobutane pyrimidine dimers; DHAD, dihydroxyacid dehydratase; DNA, deoxyribonucleic acid; ESR, electron spin resonance; FADH2, flavin adenine dinucleotide; LMCT, ligand to metal charge transfer; MDA, malonaldehyde; NADH, nicotinamide adenine dinucleotide; NER, nucleotide excision repair; NOM, natural organic matter; PET, polyethylene tetrapthalate; POM, particulate organic matter; PP, photoproduct; ROS, reactive oxygen species; SOD, superoxide dismutase; SODIS, solar disinfection; tRNA, transfer ribonucleic acid; UV, ultraviolet (light); Vis, visible (light).

* Corresponding author at: SB, ISIC, GPAO, Ecole Polytechnique Fédérale de Lausanne (EPFL), Station 6, 1015 Lausanne, Switzerland.
** Corresponding author at: Plataforma Solar de Almería – CIEMAT, P.O. Box 22, Tabernas, Almería, 04200, Spain.
E-mail addresses: pilar.fernandez@psa.es (P. Fernández Ibáñez), cesar.pulgarin@epfl.ch (C. Pulgarin).

http://dx.doi.org/10.1016/j.apcatb.2016.06.009
0926-3373/

1. Chapter I: Introduction

The year 1894 marked a new era in chemistry, with the postulation of the so-called Fenton reaction, named after H.J.H. Fenton himself. Although accidentally, it was found that iron ions, when combined with oxidizing agents, resulted in a solution with higher oxidative capacities than its separate components. The first "application" was the mix of hydrogen peroxide, tartaric acid, a base and iron (II) salt [1]. The identification of this finding marked the "Fenton reaction" or "Fenton reagent" and the first full publication which he authored indicated the principles of what we refer today as Fenton chemistry [2]:

1) The use of an oxidant,
2) a metal in its reduced form and
3) the involvement of higher oxidation state of the used metal.

Although the initial formulation involved the application of iron (II) and H_2O_2 or hypochlorous acid, nowadays, we know that many metals can be used to facilitate the reaction, involving Cu, Cr, V, Ni, persulfate and/or organic peroxides can participate, and the H_2O_2 can be replaced by chlorine water or CaO_2 [1,3–5].

Fenton himself continued his research using this reaction for the synthesis of hydroxylated compounds. The years that followed were governed by controversy on the action mode of this reaction, such as Bray and Gorin [6] who proposed the involvement of ferryl species $[Fe(IV)O]^{2+}$ or Haber and Weiss [7], who proposed the one-electron oxidation of H_2O_2, and other investigators [8] who suggested that the free radical mechanism is not plausible, but other intermediates are involved.

The progress continued with additions (from Baxendale et al. and Barb et al.) [9,10] and better understanding of the process led to the Fenton treatment of various effluents from industrial activities. Walling contributed significantly to the understanding of the process against pollutants [11–16], but the treatment of microorganisms was still out of question. No one could imagine that the massive wastewater flows could be acidified for disinfection of microorganisms. Nevertheless, investigators such as Irwin Fridovich and James Imlay, have contextualized the Fenton reaction and its significance to biological systems (*e.g.* Imlay et al.) [17], and the first notions of its importance have been made. One hundred years after the discovery, unanimity prevailed over the importance of the Fenton reaction in chemistry and biology.

The modern era in photo-Fenton started during the 90's, when the first trials at higher pH were initiated [18], and the contextualization assays of the photo-Fenton reaction were set-up [19–21]. The first effort to inactivate microorganisms with iron complexes was made by Cho et al., [22] and the first actual near-neutral photo-Fenton reaction for microorganisms' inactivation was performed by Rincon and Pulgarin two years later [23]. The enhancing effect of the photo-Fenton process for *E. coli* inactivation in drinking water was for the first time reported, opening the way for new research directions; the near-neutral photo-Fenton works targeting various microbiological pollutants are presented in Table 1. These past 10 years, until now, have witnessed numerous works in micro-contaminant and microbiological pollutant elimination.

In this review, we present a holistic approach to the (solar) photo-Fenton-driven inactivation of bacteria, and move from the entirely internal processes towards the external events that take place in aqueous media. More specifically, we begin with the direct effects of light on microorganisms, on their vital components, separating the direct (Chapter II) and the indirect actions of light (Chapter III). A conceptual review of the various actions, focusing on the photo-biological aspects is performed. As the photo-Fenton process is a synergetic sum of different parts based on light exposure, it is in fact a solar disinfection which can be enhanced (Chapter IV), either by H_2O_2, by iron, or both simultaneously; the effects of each process are deeply discussed. The final chapter (Chapter V), deals with the basic interactions of the aqueous media in which solar photo-Fenton may take place. Critical points and details on the effects that simultaneously occur, and elucidation of the process in a high degree is provided to the reader.

Table 1
Chronological review of the works on near-neutral photo-Fenton inactivation of microorganisms.

Authors	Year	Reference	Topic
Cho et al.	2004	[22]	Inactivation of *Escherichia coli* by photochemical reaction of ferrioxalate at slightly acidic and near-neutral pHs
Rincon and Pulgarin	2006	[23]	Comparative evaluation of Fe^{3+} and TiO_2 photoassisted processes in solar photocatalytic disinfection of water
Rincon and Pulgarin	2007a	[24]	Absence of *E. coli* regrowth after Fe^{3+} and TiO_2 solar photoassisted disinfection of water in CPC solar photoreactor
Rincon and Pulgarin	2007b	[25]	Fe^{3+} and TiO_2 solar-light-assisted inactivation of *E. coli* at field scale
Moncayo-Lasso et al.	2008	[26]	Bacterial inactivation and organic oxidation *via* immobilized photo-Fenton reagent on structured silica surfaces
Moncayo-Lasso et al.	2009	[27]	Simultaneous *E. coli* inactivation and NOM degradation in river water *via* photo-Fenton process at natural pH in solar CPC reactor. A new way for enhancing solar disinfection of natural water
Kim et al.	2010	[28]	*Inactivation of MS2 Coliphage by Fenton's reagent*
Mazille et al.	2010	[29]	Comparative evaluation of polymer surface functionalization techniques before iron oxide deposition. Activity of the iron oxide-coated polymer films in the photo-assisted degradation of organic pollutants and inactivation of bacteria
Sciacca et al.	2010	[30]	Dramatic enhancement of solar disinfection (SODIS) of wild Salmonella sp. in PET bottles by H_2O_2 addition on natural water of Burkina Faso containing dissolved iron
Spuhler et al.	2010	[31]	The effect of Fe^{2+}, Fe^{3+}, H_2O_2 and the photo-Fenton reagent at near neutral pH on the solar disinfection (SODIS) at low temperatures of water containing *Escherichia coli* K12
Nieto-Juarez et al.	2010	[32]	*Inactivation of MS2 coliphage in Fenton and Fenton-like systems: role of transition metals, hydrogen peroxide and sunlight*
Sciacca et al.	2011	[33]	Solar disinfection of wild *Salmonella sp*. in natural water with a 18 L CPC photoreactor: Detrimental effect of non-sterile storage of treated water
Bandala et al.	2011	[34]	Application of azo dyes as dosimetric indicators for enhanced photocatalytic solar disinfection (ENPHOSODIS)
Bernabeu et al.	2011	[35]	*Exploring the applicability of solar driven photocatalytic processes to control infestation by zebra mussel*
Ortega-Gomez et al.	2012	[36]	Water disinfection using photo-Fenton: Effect of temperature on *Enterococcus faecalis* survival
Moncayo-Lasso et al.	2012	[37]	The detrimental influence of bacteria (*E. coli, Shigella and Salmonella*) on the degradation of organic compounds (and vice versa) in TiO_2 photocatalysis and near-neutral photo-Fenton processes under simulated solar light.
Polo-Lopez et al.	2012	[38]	*Mild solar photo-Fenton: An effective tool for the removal of Fusarium from simulated municipal effluents*
Klamerth et al.	2012	[39]	Treatment of Municipal Wastewater Treatment Plant Effluents with Modified Photo-Fenton As a Tertiary Treatment for the Degradation of Micro Pollutants and Disinfection
Garcia-Fernandez et al.	2012	[40]	Bacteria and fungi inactivation using Fe^{3+}/sunlight, H_2O_2/sunlight and near neutral photo-Fenton: A comparative study
Bandala et al.	2012	[41]	*Inactivation of Ascaris eggs in water using sequential solar driven photo-Fenton and free chlorine*
Rodriguez-Chueca et al.	2013	[42]	Inactivation of *Enterococcus faecalis, Pseudomonas aeruginosa* and *Escherichia coli* present in treated urban wastewater by coagulation-flocculation and photo-Fenton processes
Ortega-Gómez et al.	2013	[43]	Inactivation of *Enterococcus faecalis* in simulated wastewater treatment plant effluent by solar photo-Fenton at initial neutral pH
Nieto-Juarez and Kohn	2013	[44]	*Virus removal and inactivation by iron (hydr)oxide-mediated Fenton-like processes under sunlight and in the dark*
Ndounla et al.	2013	[45]	Inactivation by solar photo-Fenton in PET bottles of wild enteric bacteria of natural well water: Absence of re-growth after one week of subsequent storage.
Agulló-Barceló et al.	2013	[46]	Solar Advanced Oxidation Processes as disinfection tertiary treatments for real wastewater: Implications for water reclamation
Rubio et al.	2013	[47]	Comparative effect of simulated solar light, UV, UV/H_2O_2 and photo-Fenton treatment (UV–vis/H_2O_2/$Fe^{2+,3+}$) in the *Escherichia coli* inactivation in artificial seawater
Polo-Lopez et al.	2013	[48]	*Benefits of photo-Fenton at low concentrations for solar disinfection of distilled water. A case study: Phytophthora capsici*
Ruales-Lonfat et al.	2014a	[49]	Iron-catalyzed low cost solar activated process for drinking water disinfection in Colombian rural areas
Ruales-Lonfat et al.	2014b	[50]	Deleterious effect of homogeneous and heterogeneous near-neutral photo-Fenton system on Escherichia coli. Comparison with photo-catalytic action of TiO_2 during cell envelope disruption
Ndounla et al.	2014a	[51]	Evaluation of the efficiency of the photo Fenton disinfection of natural drinking water source during the rainy season in the Sahelian region
Ndounla et al.	2014b	[52]	Relevant impact of irradiance (vs. dose) and evolution of pH and mineral nitrogen compounds during natural water disinfection by photo-Fenton in a solar CPC reactor.
Ortega-Gómez et al.	2014a	[53]	Solar photo-Fenton for water disinfection: An investigation of the competitive role of model organic matter for oxidative species
Ortega-Gómez et al.	2014b	[54]	Inactivation of natural enteric bacteria in real municipal wastewater by solar photo-Fenton at neutral pH

Table 1 (*Continued*)

Authors	Year	Reference	Topic
Teodoro et al.	2014	[55]	Disinfection of greywater pre-treated by constructed wetlands using photo-Fenton: Influence of pH on the decay of *Pseudomonas aeruginosa*
Rodríguez-Chueca et al.	2014a	[56]	Disinfection of wastewater effluents with the Fenton-like process induced by electromagnetic fields
Rodríguez-Chueca et al.	2014b	[57]	Disinfection of real and simulated urban wastewater effluents using a mild solar photo-Fenton
Polo-Lopez et al.	2014	[58]	*Assessment of solar photo-Fenton, photocatalysis, and H_2O_2 for removal of phytopathogen fungi spores in synthetic and real effluents of urban wastewater*
Ruales-Lonfat et al.	2015	[59]	Iron oxides semiconductors are efficients for solar water disinfection: A comparison with photo-Fenton processes at neutral pH
Giannakis et al.	2015	[60]	Ultrasound enhancement of near-neutral photo-Fenton for effective E. coli inactivation in wastewater
Ortega-Gómez et al.	2015	[61]	*Principal parameters affecting virus inactivation by the solar photo-Fenton process at neutral pH and μM concentrations of H_2O_2 and $Fe^{2+}/^{3+}$.*
Barreca et al.	2015	[62]	*Escherichia coli* inactivation by neutral solar heterogeneous photo-Fenton (HPF) over hybrid iron/montmorillonite/alginate beads
Pulgarin C.	2015	[63]	Fe vs. TiO_2 photo-assisted processes for enhancing the solar inactivation of bacteria in water.
Ndounla and Pulgarin	2015	[64]	Solar light (hv) and H_2O_2/hv photo-disinfection of natural alkaline water (pH 8.6) in a compound parabolic collector at different day periods in Sahelian region
Rodríguez-Chueca et al.	2015a	[65]	Kinetic modeling of *Escherichia coli* and *Enterococcus* sp. inactivation in wastewater treatment by photo-Fenton and H_2O_2/UV–vis processes.
Rodríguez-Chueca et al.	2015b	[66]	Conventional and Advanced Oxidation Processes Used in Disinfection of Treated Urban Wastewater
Aurioles-López et al.	2015	[67]	*Effect of iron salt counter ion in dose–response curves for inactivation of Fusarium solani in water through solar driven Fenton-like processes*
Ruales-Lonfat et al.	2016	[68]	Bacterial inactivation with iron citrate complex: A new source of dissolved iron in solar photo-Fenton process at near-neutral and alkaline pH
Ruiz-Aguirre et al.	2016	[69]	Assessing the validity of solar membrane distillation for disinfection of contaminated water
Ortega-Gómez et al.	2016	[70]	Wastewater disinfection by neutral pH photo-Fenton: The role of solar radiation intensity
Giannakis et al.	2016a	[71]	*Castles fall from inside: Evidence for dominant internal photo-catalytic mechanisms during treatment of Saccharomyces cerevisiae by photo-Fenton at near-neutral pH*
Giannakis et al.	(under review)		Micropollutant degradation, bacterial inactivation and regrowth risk in wastewater effluents: influence of the secondary (pre)treatment on the efficacy of Advanced Oxidation Processes

2. Chapter II: Direct action of light

2.1. UVB wavelengths (290–320 nm) effect

The germicidal action in the solar disinfection of drinking water is attributed to the wavelengths reaching the Earth's surface. Although UVC is absorbed during its passage through the atmosphere and can be neglected, UVB is very often not taken into account, when the physical and microbiological aspects of the process are estimated. This strategy may be true for SODIS taking place in recipient vessels which filter UVB, but before its diminution due to path length limitations, UVB affects significantly a considerable layer of the exposed natural water bodies, mainly leading to mutations and possibly apoptosis and/or imminent cell death. The significance of this process has been long identified [72] and has influenced the design of solar disinfection units [73]; the UVB germicidal effect is 100–1000 times more efficient against microbial inactivation than UVA. Hence, this chapter of the present review is dedicated to the biological effects of the direct UVB action on bacteria (Fig. 1).

In principle, UVB inflicts damages due to its absorption by the various cellular components. More specifically, Bensasson et al. [74] offer an extensive review on the components directly damaged by UVB irradiation (for instance, chromophores like the heme groups, enzymes, vitamins, acids), with the principal targets being the genetic material and the proteins. Other components such as lipids and polysaccharides do not undergo direct damage, as their absorption in this wavelength region is limited [75]. Considering the affected entities, the damage will be separated in DNA photoproducts, targets of protein nature and iron bearing compounds. The further implications connected to the repair mechanisms will also be assessed.

2.1.1. UVB-induced DNA photoproducts

Commonly, the UVB wavelengths lead to the formation of same-strand photo-adducts among nitrogen-containing bases [76–79], or even in double stranded DNA [80]. These photoproducts fall within the next categories [78]:

2.1.1.1. Cyclobutane pyrimidine dimers (CPDs). Light excites pyrimidine bases in a triplet state, which then undergoes a [2 + 2] addition of the C5-C6 bonds of consequent pyrimidine bases, forming the *cis*-syn cyclobutane pyrimidine dimers (P<>P) [78]. This process is very similar to the effects of shortwave UVC irradiation, which leads to common photo-products [81–84].

2.1.1.2. Pyrimidine (6-4) pyrimidone dimers. Under a different energetic transition than CPDs, a pyrimidine base is excited to singlet state and reacts with another pyrimidine base, by [2 + 2] cycloaddition, forming the stable bonds, and the pyrimidine (6-4) pyrimidone dimers [78,81,84]. Further phenomena take place due to the shift of UV light absorption towards the long UV wavelengths, and the further absorption of UV (A or B) light converts these adducts into different isomers, the Dewar valence isomers [85,86]. These stereoisomers add to the existing problems of DNA replication.

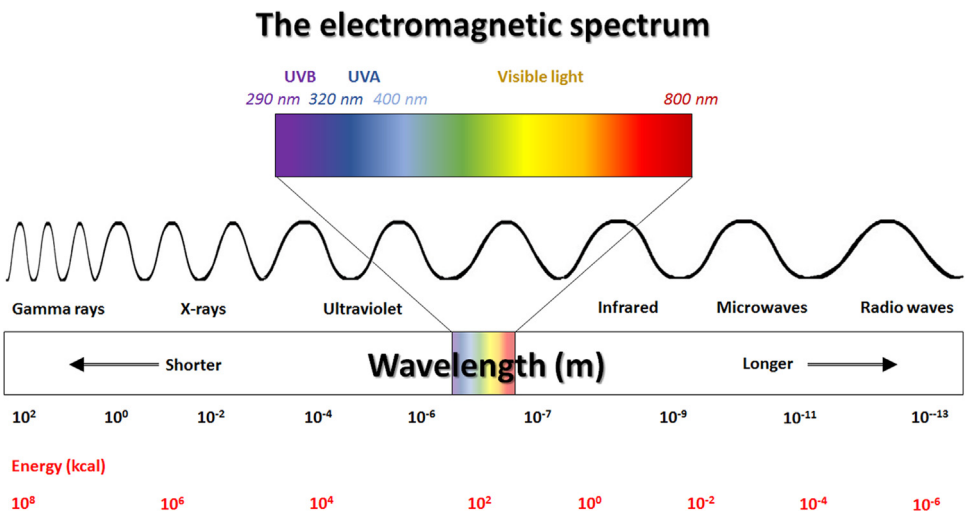

Fig. 1. The electromagnetic spectrum, with emphasis on the UV–vis light. The order of increasing wavelengths, as well as the decreasing energy are noted.

2.1.1.3. Monomeric pyrimidine (cytosine) photoproducts. Light absorption from the monomeric cytosine compounds has been found to favor their excitation to singlet state and a subsequent nucleophilic addition of water. The hydrated product "6-hydroxy-5,6-dihydrocytosine" or cytosine photo-hydrate is formed [87].

2.1.1.4. Purine base photoproducts. Along with pyrimidine bases, purine bases share the characteristics of high UV light absoprtion at 260 nm, tailing up to the UVB region [75,85]. As a result, photo-damage is bound to take place. Dewar adducts in isolated DNA have been reported [75,88] and lesser damages include bi-stranded Oxy-Purine or abasic clusters, double strand breaks [89]. However the most common products are the T<>T, T<>C and (6-4) T<>C dimers [88].

2.1.2. Other UVB targets

While the strand itself suffers from extensive photo-damage, there are additional candidates reported in literature, such as some proteins and their constituents and other more complex targets, such as enzymes and proteins. In principle, UVA light (above 320 nm) is not absorbed by proteins without bound co-factors or groups, as they do not contain chromophoric compounds in this region [75,90]; in the opposite case, *i.e.* UVB wavelengths, this is deemed possible. However, in the case of UVB, some amino acids, such as are tryptophan (Trp), tyrosine (Tyr), phenylalanine (Phe), histidine (His), cysteine (Cys) and cysteine residues, are reported to absorb UV light (for UV spectra, see Bensasson et al. [74]). The rest of the amino acids absorb mainly at 190 nm, tailing up to 220 nm, mostly due to the presence of the peptide bond [–C(O)–NH–]. Therefore, as UVC wavelengths are not present in the solar spectrum, it is concluded that the absorption by the backbone of the proteins is negligible [90]. Another target that will be analyzed in next chapters and initiates indirect reactions is enterobactin. This powerful iron-chelating agent has peak absoprtion at 316 nm [91]. This behavior suggests chromophoric abilities and the result is an increase of the iron concentration in the cell. Finally, as a result of the cell exposure to UVB light, depending on the damage levels on the genome, either apoptosis or repair can be initiated. It can be demonstrated that cell death can be avoided by CPD restoration, by nucleotide excision repair (NER) [92,93]. However, some of the proteins (Fpg, formamidopyrimidine-DNA glycosylase) responsible for DNA repair are suspected to be prone to UVB-induced alterations, which inactivate them [94].

2.2. UVA wavelengths (320–400 nm) effect

As explained in the beginning, in the case SODIS is taking place in polyethylene terephthalate (PET) or plain glass bottles, UVA light is the principal wavelength region causing bacterial inactivation during solar exposure of water. Although differences can occur in the absorbed UVA wavelengths among the materials that carry the treated water, the largest fraction of these wavelengths will get transmitted; in PET or borosilicate bottles the absorption spectra differ in the near-UVB region, permitting a higher fraction in the latter case. Overall, the direct effects of UVA can be characterized as less harmful, compared with the rest of the UV light wavelengths, but the direct absorption by DNA, proteins and other structures is noteworthy [75,78,95,96] and will be discussed in this part. The indirect pathways will be further analyzed in later stages of this review.

2.2.1. Direct UVA DNA damage

In an analogy with UVB light, UVA is responsible of inflicting a series of different types of damage to DNA. The hypothesis on UVA-induced CPD formation [83,97,98] were verified. Besaratinia et al. [99] proved that CPDs are also formed under UVA light, but in a different way than UVB [100]. It has been reported that the photo-products are strand breaks, oxidation of pyrimidines, purines (all analyzed afterwards) and CPDs [97] in a ratio of 1:1:3:10. According to the medium carrying the DNA, the degree of damage can differ; high CPD formation is induced in pure water [101]. In the same work, and other ones (for instance Mouret et al. [102]) the direct connection of UVA-and CPDs was verified. The wavelengths that can induce the CPD formation tail up to 365 nm, both for isolated and cellular DNA [103–106], with simultaneous absence of (6-4) photo-products. Mainly, the dimerization took place among thymine bases at nearly 90% of the total dimers [102], through direct absorption of UVA light although initially a photo-sensitizer was thought to mediate [97]. Finally, the formation of the Dewar valence isomers is also attributed to UVA light absorption, as this photo-transformation peaks at around 320 nm, border among UVA and UVB light [79]. Especially (6-4) PPs produced by UVB illumination will undergo UVA-mediated conversion to an isomer [85,86,97], if the light source emits both UVB and UVA wavelengths, such as sunlight [79,107].

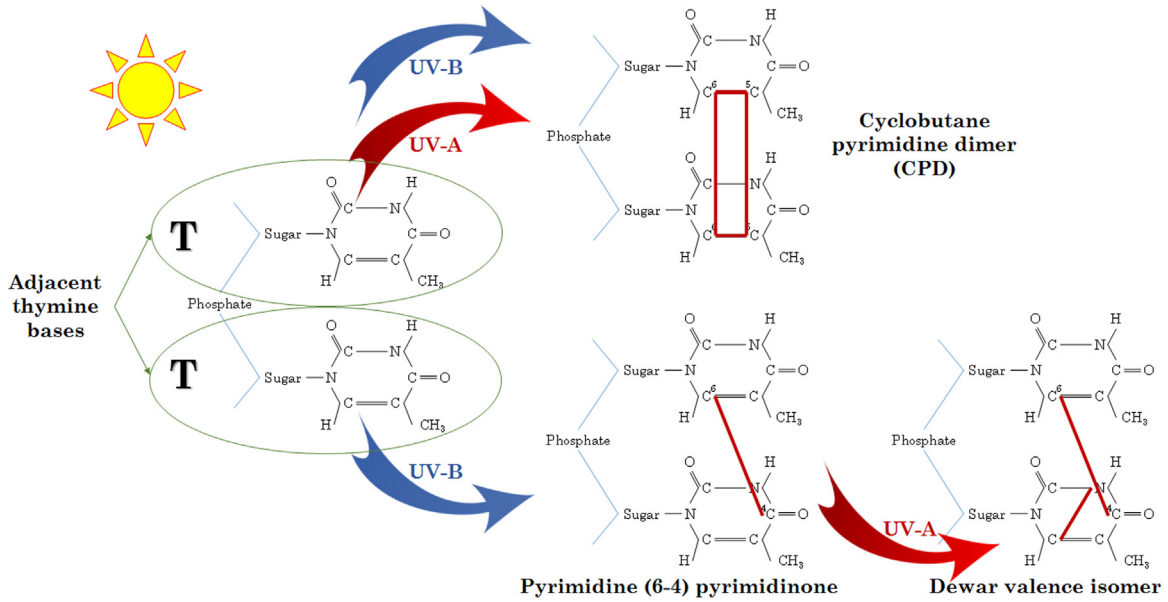

Fig. 2. Chemical structural modifications of the DNA during exposure to solar light (adapted from Batista et al. [100]). The exposure of thymine bases to light can induce the formation of CPDs and (6-4) PPs, while the existence of UVA can further inflict modifications in the structure of the chain, the Dewar valence isomers.

2.2.2. UVA oxidative damage

Although CPDs are formed in a higher ratio than the other products [97], UVA light is responsible for a series of other reactions, namely Type I and Type II photo-oxidation reactions [78,108]. Type I reactions are one-electron oxidation (or hydrogen atom abstraction) processes, and Type II are singlet oxygen (Δg^1O_2or more simply $^1O_2$) ones [75,78,109]. In Type I reactions, DNA bases are the electron donors, and especially guanine, compared with thymine, adenine, cytosine and 5-methycytosine [78]. The result of this process is a large quantity of base (guanine) cations, possibly hydrated or deprotonated afterwards. However, the excitation by UVA light, in Type II reactions, singlet oxygen is involved, reacting with electron rich bases. As a result, singlet oxygen facilitates the energy transfer from guanine towards molecular oxygen [78,110], also involving unstable stereoisomers among its C4 and C8 carbon atoms [78,111]. However, since Type II reactions are oxygen-dependent, their main action is considered indirect and will be analyzed in next chapters (Fig. 2).

2.2.3. Other UVA targets

Apart from DNA, UVA light affects other compounds in the cell with significant biological effects. More specifically, compounds that participate in either the metabolic cycle or are vital for cell homeostasis exhibit UVA absorption. Catalase, for instance, is an enzyme which regulates the H_2O_2 concentration during the respiration process, and UVA light effects suggest an inhibition of peroxidase activity [91]. Dihydroxy acid dehydratase (DHAD) is one of the iron-sulfur containing molecules, which demonstrates photo-sensible behavior and can be inactivated by irradiation [112,113]. Its modification can initiate further indirect stress; more details on the compounds that initiate indirect pathways of damage will be given in following chapters. Furthermore, the thiolated tRNA is a trigger molecule for environmental changes, which indicates possible stresses of near-UV nature [91]. Finally, ribonucleotide reductase, a key enzyme in metabolic cycles of living organisms, contains components with strong absorption in the UV range that are likely to be affected by irradiation [91].

2.3. Simultaneous UVA and UVB exposure

During simulated solar exposure, if both UVB and UVA wavelength groups are transmitted effectively through the medium, the DNA damage resembles mostly the pattern due to the UVB wavelengths [80]. After some hours under simulated solar light, the analyses revealed undetectable levels of (6-4) photoproducts [84]; therefore it was estimated that irradiation under simulated solar light yields 20–40 times more CDPs than any other photoproducts [83,84]. Also, the contribution of UVA to thymine dimer formation is not negligible, since it produces more thymine dimers, compared to UVB alone [75], in a synergistic way. Finally, the visible light wavelengths alone, around 400–450 nm, yield damage to DNA, repairable by the Fpg proteins, but the simultaneous exposure to UVB, will hamper its capabilities [114].

3. Chapter III: Indirect action of light

3.1. Indirect inactivation mechanisms: UVB or UVA-initiated, iron release-ROS generation and cellular targets

3.1.1. Overview of the indirect pathways

According to the previous chapter, the damage inflicted onto the cells and the chain of events leading to inactivation can be separated in direct and indirect pathways. This chapter describes the indirect inactivation mechanisms, limited to the ones initiated by light but continued by various intermediaries.

As far as UVB light is concerned, its main effect is the direct formation of photoproducts, as described before. However, these wavelengths can initiate secondary mechanisms, crucial to cell survival. In principle, UVB light and catalase are involved in an unexpected inactivation pathway. First, UVB light reaches the cell. Direct actions aside, catalase is activated in a dual manner, protective or toxic [115], as follows: UVB light is absorbed by catalase and is converted to reactive chemical intermediates, in order to protect the DNA from the direct action against its bases [115]. These intermediates can be easily scavenged by the normal antioxidant enzymes [116], but under light stress, this possibility is jeopardized. The damage is heavily related to the presence of oxygen, indicating an indirect, ROS-related pathway of oxidative damage,

thanks to protonation from water, against functional moieties of the cell [115]. In our opinion, this behavior confirms an early hypothesis that catalase is not the only, or a primary intracellular enzymatic defense mechanism against toxicity of UV light [117], but other mechanisms (such as the peroxidase-supported ones, or the light absorption by pigments and similar substances) exist; further details on the oxidative protection ways will be given in the following chapters.

On the other hand, UVA wavelengths affect the DNA only to a limited extent and affect the overall functions of the cell on different levels. As explained before, UVA initiates Type I or II reactions, with the latter being oxygen dependent. It is then involved in indirect mechanisms, distinguished by the initiation by chromophores or photo-sensitizers, for Type I and II, respectively [100]. Type II reactions have even been separated into two categories, minor (superoxide radical anion-) and major (singlet oxygen-related) reactions, depending on the chemical properties of the facilitator [118]. In this review, Type II reactions will not be further distinguished in minor and major. As seen in Fig. 3, the damage in this category of reactions, is a result of absorption of light by photosensitizers, and excitation to singlet state (^{1}sens*). Through intersystem crossing, relaxation and/or internal conversion the triplet state generation is induced (^{3}sens*), then energy transfer to molecular oxygen takes place plus the subsequent production of ROS. The main enabler of electron transfer is guanine, which has high reactivity with singlet oxygen [110,119]. The photosensitizing abilities of guanine must not be excluded either; the photo-oxidation of DNA appears most frequently as 8-oxo-7,8-dihydroguanine (8-oxoGua) [97]. In the same work, the evaluation of hydroxyl radical formation *via* photosensitization was also evaluated, which can induce a variety of DNA lesions.

These modes of action explain the comparative examination performed by Santos et al. [120], who compared the damage inflicted by either UVC, UVB or UVA light. It was found that the lightest damage (high survival rates and activity) was achieved under UVA light, but was induced by the highest ROS measured, as well as protein and lipid oxidation. This order was inversed for double strand breaks, as we move towards UVC light. Here, in order to further elucidate the inactivation mechanisms initiated by light, the different ROS produced and their relationship with the functional moieties of the cell, as well as the targets of damage *via* indirect pathways are further analyzed in the next subchapters.

3.1.2. Reactive oxygen species (ROS) as a part of the cell life cycle

3.1.2.1. ROS as physiological intermediates. ROS are a natural part of the respiratory cycle of bacteria [121], when growing in aerobic conditions. The prevailing ROS formed in a trivial way are the superoxide anion () and hydrogen peroxide (H_2O_2) [122]. The process can be simplified as a spontaneous oxidation of redox enzymes, playing the role of reductants, by molecular oxygen. Since oxygen is uncharged, its presence inside the cell is unambiguous, and its internal concentration can be regarded equal to the external one [123]. The main reductants that have been identified so far are flavoenzymes [124], which facilitate transfer of electrons onto secondary compounds. A possible path includes oxygen collision with a reduced flavoenzyme, resulting in electron transfer from FADH2 [122]. With the abundance of (both oxygen and) flavins, these ROS are produced in a relatively steady quantity [125].

In *in vitro* tests, it has been found that O_2^- and H_2O_2 also form during electron transport between reductant substances and oxygen [126–129]; therefore it can be concluded that the possible reactions involve both one- and two-electron transfer [129,130]. The transfer is always completed in single steps, first by reaction of flavins with oxygen and formation of O_2^- and flavosemiquinone [122]. This product can either further react with oxygen (further forming O_2^-) or more commonly, the formed O_2^- and the flavosemiquinone further react, finally forming H_2O_2, rather than O_2^- [122].

3.1.2.2. ROS imbalance in cells. Normally, bacteria contain regulators of ROS to counter potential imbalances generated within the cells or withstand the ROS production by enzyme auto-oxidation [125]. The most known defense lines are catalase [122], Ahp Alkyl hydroperoxide reductase [131] superoxide dismutases (FeSOD, MnSOD), hydroperoxidases (HPI, HPII) and glutathione reductase (GR) [132] (Fig. 4).

Catalase is the enzyme mainly responsible for the decomposition of H_2O_2 in water and oxygen [133]. Also, Ahp Alkyl hydroperoxide reductase scavenges the normally produced H_2O_2 in *E. coli*. H_2O_2 itself is not an immediate threat to DNA (it may only cause oxidation of adenine) [134], but it engulfs the danger of hydroxyl radical production [135]. However, H_2O_2 accumulation can be detrimental to cell survival, as it will be analyzed later. Superoxide dismutases (Mn, Fe- or CuZn-SOD) are the enzymes burdened with the dismutation of O_2^- to O_2 and H_2O_2 [136]. They are located in both cytoplasm and periplasm of the cell [125]. Functionwise, they are similar, but the diffusion limitation of O_2^- at neutral pH [137,138] imposes their presence in both places. The superoxide radical itself is relatively unreactive towards DNA but can participate in a variety of biochemical reactions away from it. Among others, it can cause peroxynitrite formation [139,140], thymine reduction and oxidation of transition metals. Also, superoxide can react with H_2O_2 and result in the production of hydroxyl radicals [132]. Finally, peroxidases mainly dehydrogenate (by H_2O_2) phenolic and endiolic compounds, but are also responsible for the reduction of O_2 to $O_2^{\bullet-}$ and H_2O_2, using dihydroxyfumarate or NADH [141]. It has been mentioned however, that some other microbes use reductases and peroxidases, rather than dismutase and catalase, respectively, for effective internal ROS scavenging [122].

When solar light is provided to the bacterial cells, the chain reaction of events follows a complex mechanism, initiated by two simultaneous fronts: action of light and action of ROS. Assuming that a cell is preserving its normal ROS cycle, light addition creates a chain of oxidative events. UVB was mentioned to affect catalase functions, and therefore enhance H_2O_2 accumulation. It also induces excess O_2^- production in *E. coli* cells *in vivo* [142,143]. Also, singlet oxygen ($^1O_2$), key factor in cytotoxicity and gene expression [144–146] can be generated by UVA irradiation, through excitation of chromophoric substances, such as porfyrins [146].

As it seems, there is an over-accumulation of ROS inside the cell, which is only made worse by the inactivation of the key enzymes by the action of light; CAT and SOD reduce significantly their activity when exposed to UVB or UVA light [120,122,125]. It has long been suggested that near-UV induces mutations in bacteria (in macroscopic level) and the explanation has been attributed to the excess H_2O_2 accumulated into the cell and the subsequent reactions involved with it [91]. UVA has also been known to affect the respiratory chain of *E. coli*, with some of the mechanisms suggested by Bosshard et al. [121] being verified in this cycle of events. A malfunctioning electron transport chain would provide electrons, with many reductants now available to accept them and convert themselves to reactive intermediates. Also, the oxidizing agents' accumulation will lead to ROS production by internal metal- and NAD(P)H-driven reactions [147]; the reductants will act towards the regeneration of the catalysts of these reactions. Therefore, at this point, it is important to analyze the release of metals and their result.

3.1.3. The significance of the internal Fenton process: iron release and facilitation

3.1.3.1. Physiological state of iron into the cell. Iron homeostasis in bacterial cells is controlled and kept in physiological levels by the

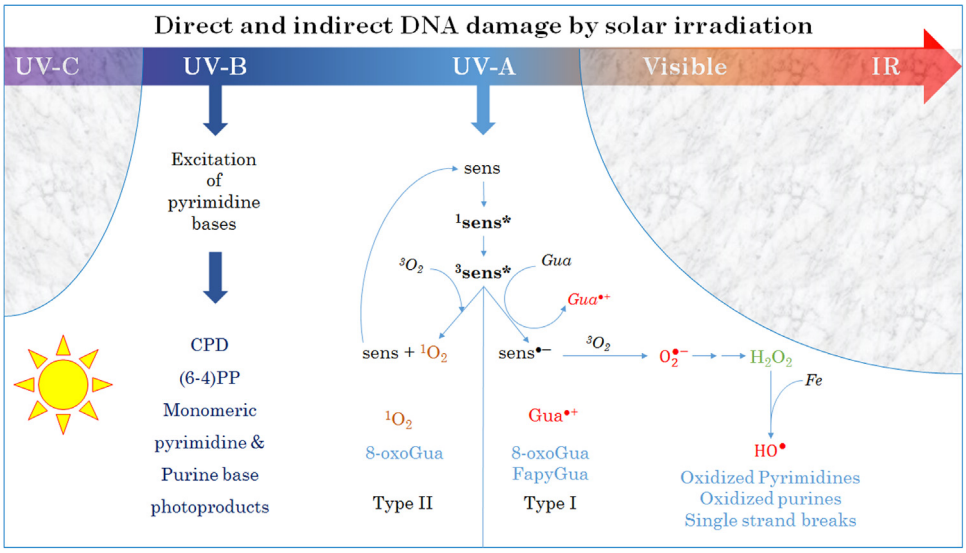

Fig. 3. Direct and indirect DNA damage mechanisms (adapted from Cadet et al. [386]). The different pathways initiated from UVB and the Type I and II induced by UVA are depicted, limited to the DNA damage as end-product.

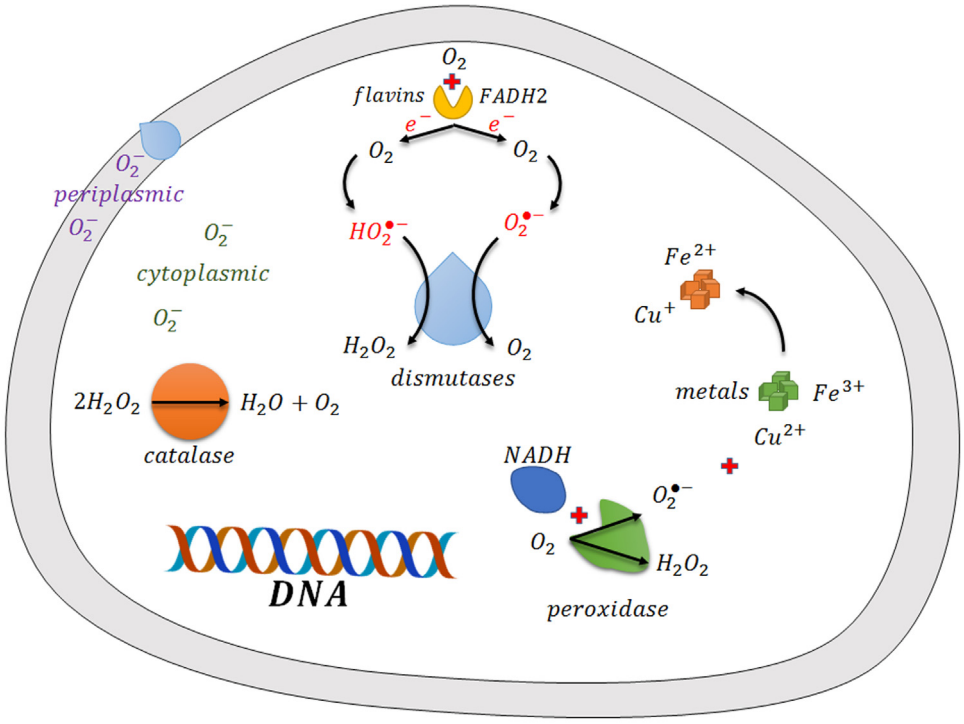

Fig. 4. Internal ROS cycle, before light addition. The opportunistic creation of ROS is depicted here, with the pair of superoxide radical anion ($O_2^{\bullet-}$)/hydroperoxyl radical ($HO_2^{\bullet-}$) being the most reactive species. Their scavenging efficiency determines the auto-damage levels, *via* direct damage (oxidation) or indirect creation of more reactive ROS in reduced-metal catalyzed reactions with H_2O_2.

Fur protein. It is the most common iron regulator (among others) in bacteria [148], controlling the genes implicated in iron acquisition, but also de-repression of the genes during iron deprivation [149]; the genes which encode proteins concerning direct Fe^{2+} acquisition or the transfer of Fe^{3+} by siderophoric action are negatively regulated by Fur [150,151], acting as a repressor of transcriptional activity [149]. Fe^{2+} is soluble enough to feed the growth needs of bacteria, but the problems are found with Fe^{3+}. Usually, it is solubilized by siderophores produced by bacteria, chelating and efficiently delivering Fe^{3+}. Especially in near-neutral conditions, the aqua-complexes of Fe^{3+} are insoluble in water [152], and the siderophoric action facilitates their use. In total, bacteria utilize many transport systems to satisfy their needs; for instance, *E. coli* K-12 use 7 transport systems. Interestingly, although the siderophore movement through the outer membrane is excluded due to the size of the protein, the gram-negative bacteria tend to use the outer surface receptor proteins as transport ones [153].

Internally, iron in *E.coli* is contained in components such as bacterioferritin and ferritin [153–156]. Ferritin is essentially an iron storage unit, with a molecular weight of 444.000 kDa and 4500 mol Fe/mol protein. Its structure is complex, consisting of 24 sub-units, a protein surface cover (apoferritin) and 6 places for

interior communication. Its function consists in storage of "free", non-protein-bound iron into the cell, oxidizing the Fe^{2+} with the aid of proteins [157]. On a reverse function, it can release Fe^{2+} from the stored Fe^{3+} by the use of reducing biological compounds. This function is crucial for the cell, but it can provide a potential target for the oxidants accumulated into the cell during oxidative stress. Also, other iron containing units are the Fe/S clusters. Dehydratases contain [4Fe-4S] clusters which include readily soluble iron atoms, prone to oxidation as well [155]. Finally, iron can also bind to the surface of the DNA structure and specifically, it is chelated to the phosphodiester backbone [17].

3.1.3.2. Light-induced changes in iron homeostasis. During light exposure, iron is playing a key role in the subsequent oxidative stress. There are two possible ways of iron release into the cell: the ROS-mediated and the direct damage to the iron containing compounds.

The ROS production, as described in the previous chapter can play the role of the intermediate, which "unlocks" the structures and releases iron into the cell. More specifically, the superoxide anion can extract iron from the iron-storage proteins [158–161], through oxidation of dehydratases, for instance. As described before, the critical iron atom is bound and the cluster is left in an unstable state [125]; the $[4Fe\text{-}4S]^{2+}$ form is univalently oxidizing the cluster to $[4Fe\text{-}4S]^{3+}$, resulting into released ferrous iron and $[3Fe\text{-}4S]^{+}$ cluster [161,162]. Hydrogen peroxide causes similar damage [163] by a two-step process, releasing ferric iron and the same $[3Fe\text{-}4S]^{+}$ cluster [162]. The simultaneous production of "free" iron, H_2O_2 and superoxide radical anion which can reduce Fe^{3+} to Fe^{2+} [17], can effectively facilitate an internal Fenton reaction.

As far as the light itself is concerned, the previous actions simply aggravate. Near UV is known to degrade membrane structures inside the cell [164]. More specifically, Fe/S clusters absorb in the UVA region [112]. UVA has been found to degrade ferritin and other ferritin-like substances, leading to immediate release of iron into the cytoplasm [146,165,166] *via* destruction of its ligand [112]. Most importantly, in presence of these chelating ligands and ROS, the Fenton reaction is already taking place, producing $HO^{\bullet}$. Taking into account the incident light in these wavelengths, the Fenton reaction will find its catalyst regenerated back to Fe^{2+} with the simultaneous production of another hydroxyl radical.

3.1.4. Internal targets of the oxidative damage

Light action against the cell presents a uniformity in its application, if saturation conditions are applied. Although some compounds demonstrate a photo-absorbing activity, it is rather unlikely that shading occurs significantly, if no physical barriers exist. However, this statement does not stand equally true for the ROS damage during oxidative stress conditions, since ROS are short living, and in their majority, diffusion limited. Therefore, except for the long-living H_2O_2 and O_2^- the rest cause "local" damage. The effects can be separated according to the mediator (ROS) or the target; here, the latter is going to be presented, separating the damage on the DNA, and the rest of the involved compounds (proteins, enzymes, lipids etc).

3.1.4.1. Oxidative-driven DNA damage. DNA was long identified as a weak link in the chain of resistance to ROS damage by light-initiated internal Fenton reactions, for two main reasons: it was mentioned that it can effectively bind loose iron [17,75] catalyzing the Fenton reaction and suffering oxidative damage at the site of reaction. Then, the possibility of withholding such damage is considerably more crucial to survival than in other components of the cell [17]. Diffusion-limited oxidative damage by $HO^{\bullet}$ can induce different effects, such as base oxidation, sites which suffer base loss, inter-strand adducts within DNA, DNA-protein crosslinks and ultimately, DNA strand breaks [134,135,167–169]. Strand breaks are a major consequence of the reaction with $HO^{\bullet}$ [170], since the reaction with deoxyribose leads to base loss, as well as with thymine [17,171].

The hydroxyl radicals are non-selective in their mode of action. Their reaction with purine bases leads to C8-hydroxylated radical, which increases 8-oxoGua, FapyGua, 8-oxoAde and FapyAde [165]. Also, their reaction at the C5-C6 double bond ends up in the thymine and cytosine and uracil methyl oxidation by-products, 5,6-dihydroxy-5,6-dihydrothymine, 5,6-dihydroxy-5,6-dihydrocytosine and hydroxymethyluracil and 5-formyluracil, respectively [172]. Finally, hydrogen abstraction from 2-deoxyribose moieties yields strand breaks end-products [172]. Less reactive ROS, such as singlet oxygen, react with nucleotide bases at different reaction rate constants (k) reported [173]. It is noteworthy that the most prone base is again guanine, and the final damage by-product is the 8-oxo-Gua. Furthermore, ROS can attack the sugars of the DNA, with a variety of end-products actually formed [174]. The final result is lesions which are either misread by repair enzymes or block this process; the latter type leads to growth impairment and cell death [175] (Fig. 5).

3.1.4.2. Other cellular targets (proteins, lipids, membranes, Fe/S clusters). One of the first and major targets of oxidative stress during light exposure of bacteria are proteins [175]. Although it was long believed that DNA damage and lipid peroxidation are the main effects of oxidative stress, proteins have arisen as important points of interest [176]. Both $HO^{\bullet}$ and $^1\Delta gO_2$ have been reported to inflict severe and diverse problems onto the normal protein functions. Firstly, there are functional modifications in proteins, onto amino acids and protein side chains [132]. Proteins suffer from structural modifications and aggregation [177], carbonylation etc [178]. Modifications in sulfur groups (oxidation of sulfhydryl groups or reduction of disulfides), as well as oxidation of amino acids due to hydroxyl radicals, protein agglutination and cross-linking, aldehyde reactions and fragmentation of peptides have also been reported [179–184]. Especially, proteins involved in the respiration process are in danger, such as F1F0 ATPase and respiratory enzymes [178]. Modification of 3-D structure [185,186] changes in metal binding properties, susceptibility towards proteolysis and unfolding [75] should also not be excluded. Protein modifications' effects can vary from mild to severe, inducing irreversible damage to the cell [178], including cellular metabolism failures [132], membrane modifications (loss of function) [187], blocking of DNA replication, mutations [179] etc.

Singlet oxygen is not as reactive as the hydroxyl radical, but has a much longer half-life time. Its ability to affect protein functions makes it as a potentially dangerous agent, as it can react with amino acids directly. It reacts with tryptophan, tyrosine, histidine, methionine, cysteine and cysteine residues [75]. It is also responsible for inactivating enzymes, forming protein peroxides or side-chain by-products, fragmenting the backbone, as well as causing cross linking and aggregation [90]. Many functions undergo a similar effect as with the hydroxyl radical, proving its significance. Also, if not destroyed, singlet oxygen can affect the properties of the protein, such as its turnover efficiency [90]. Proteins are also in danger from the indirect pathway triggered by hydrated electrons, which add to molecular oxygen, produce $O_2^{\bullet -}$ and can subsequently damage proteins [75].

Moving to even more inert ROS, O_2^- and H_2O_2 can affect other groups, such as Fe/S dehydratases or mononuclear Fe-enzymes [175]. Superoxide is less harmful although more reactive than H_2O_2 [122] and acts mostly in blocking the [4Fe-4S] clusters as described before; the inactivation of dehydratases causes pathway failure. H_2O_2 on the other hand, can oxidize sulfur atoms (oxidation of cystenyl residues, or oxidation of sulfinic moieties) [122], or (through

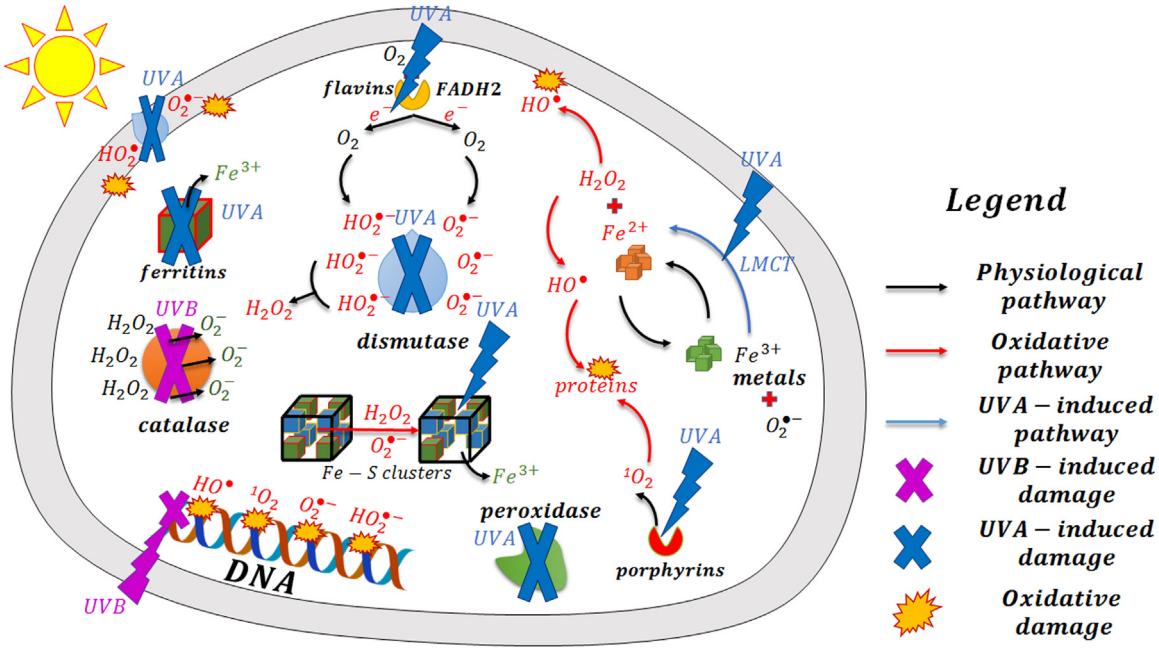

Fig. 5. Light induced changes in cell homeostasis. a) UVB-induced damage to DNA and CAT functions, b) UVA affects the functions of enzymes and proteins related with the ROS production (flavins, FADH2, CAT, SOD, peroxidases, porphyrins), leading to accumulation of ROS, c) release of iron and reduction by light, d) LMCT-driven reduction of iron and internal photo-Fenton initiation.

$HO^{\bullet}$ in the Fenton process) carbonylate proteins, and oxidize Fe/S clusters [122].

Finally, although some of the targets presented seem like end-products, there are significant side-products possibly forming, inducing secondary damage [75]. For instance, the peroxides formed on proteins and peptides can cause oxidation of residues on other proteins or deplete antioxidants [188], or even increase the possibility of DNA-base oxidation [189], with the consequences already analyzed before (*i.e.* strand breaks and DNA-protein adducts).

The second large group of substances undergoing damage is lipids and fatty acids. A proposed chain reaction of autocatalytic lipid peroxidation has been proposed [170], where oxidation by $HO^{\bullet}$ leaves a lipid radical anion readily reacting with molecular oxygen to form lipid peroxyl radicals. These radicals can potentially play the role of $HO^{\bullet}$ in the next cycle, and trigger an auto-oxidation process. Metals and H_2O_2 can generate the necessary $HO^{\bullet}$, while singlet oxygen [146] or the secondary damage by protein photoproducts could initiate the peroxidation process. Some authors have suggested the dangers of lipid peroxidation [121,190] but in order to facilitate this reaction, the bacteria must contain the polyunsaturated lipids; it is suggested that most membranes lack these compounds [121].

4. Chapter IV: Enhancements

4.1. Hydrogen peroxide (H_2O_2)

In the previous chapters, we have reviewed the actions that take place during sole irradiation of bacteria by light, including UVB, UVA and visible light. The various mechanisms that have been described, lead to the assertion that the main mechanisms of cellular inactivation by light are two: direct light action (mutations, strand breaks etc.) and indirect light-initiated pathways (ROS formation, iron release and the subsequent internal Fenton and photo-Fenton reactions). During the ROS formation, superoxide and H_2O_2 have been found critical in the facilitation of the internal photo-Fenton reaction, in both direct damage to bio-molecules and indirect aggravation of ROS production. In this chapter, we assess the enhancement of photo-inactivation of bacteria, by the simple addition of H_2O_2, and present the mechanisms that take part internally and externally, in absence or presence of light.

4.1.1. H_2O_2 actions, in absence of light

Hydrogen peroxide (H_2O_2) is a relatively strong oxidant, with potential 1.8 V at pH = 0 and 0.87 V at pH = 14 [191]. In natural waters, its formation is connected with photochemical mechanisms, explained in next chapters of the review, or the release of metals and sulfur from anoxic regions [192]; when near-neutral conditions are encountered, the expected potential is around 1.4 V. The use of H_2O_2 in biological-related activities was connected with disinfection and biofilm growth control [191].

As analyzed in the previous chapter, intracellular H_2O_2 is a normal by-product of the respiration process, through the auto-oxidation of respiratory dehydrogenases of bacteria [122], which in turn can regulate and maintain these ROS concentrations to nanomolar levels, by catalases and peroxidases [193]. However, if the H_2O_2 is present in the surroundings of the microorganism, since it is an uncharged molecule, it is known to diffuse through membranes, therefore facilitating its transport into the cell [193]. Therefore, a steady state concentration is preserved, as a balance of its intracellular generation, the potential diffusion from outer sources and the scavenging efficiency from the enzymes [194]. Different physiological states can imply varying steady state concentrations [195]. The imbalance created into the cell can either be scavenged or inactivate enzymes; reports mention 20% of the external concentration of H_2O_2 is able to diffuse into the cell [193], ultimately leading to cell death. In order to separate the different pathways with which H_2O_2 can lead to cell inactivation, the lieu and the mode will be assessed.

Beginning with the external actions, as H_2O_2 can be either naturally produced or voluntarily added, a wide range of concentrations can be encountered. Imlay and Linn [196] have experimented with mM concentrations of H_2O_2, and a correlation between H_2O_2 addition and cell inactivation was confirmed [17,196]. Two main categories of concentrations can be suggested: low (1–3 mM) H_2O_2

and high concentrations (> 20 mM). Internal and external damage, respectively, was reported for the two categories, namely Mode I and Mode II [197]. Mode II involves external H_2O_2 reacting probably directly with the cellular membrane, thus increasing its permeability; this increase can permit the inflow of extra concentrations of H_2O_2, as well as an overall detrimental impact on the viability of the cell [198]. A proportionality has been reported up to 100 mM [196].

However, the actions implicated in Mode I damage are far more intriguing. In summary, these actions are enhancing the internal Fenton reaction as it was presented in the previous chapter. More specifically, it was evidenced in [199] that μM concentrations disrupted catabolic and biosynthetic functions of the cell, by the destruction of Fe/S clusters [155,162,200,201]. The damaged cluster contributes to loose iron release and the excess of H_2O_2 will initiate Fenton reactions. However, H_2O_2 is not the only oxidant, but can act as a scavenger of electrons. More specifically, through one-electron transfer, hydroxyl radicals ($HO^{\bullet}$) can be generated. Also, *via* either direct or indirect pathways, Mode I killing will take place [196]. However, H_2O_2 can scavenge $HO^{\bullet}$, leading to the creation of the less reactive superoxide anion [196], which has a lower oxidative potential, but is biologically significant, because of its strong affinity with bacterial components [157]; moreover, it is far more long-living than $HO^{\bullet}$. Therefore, there are interesting Fenton-related implications involved, if a considerable amount of H_2O_2 is added to the bulk and saturation conditions are to be taken into account.

A very interesting concept has also been discussed in literature, concerning the nature and significance of the Fenton reaction itself [199,202,203], and more specifically, the effect of the reaction kinetics. The k constant for the oxidation of Fe^{2+} at pH values around 3 is 76 M^{-1}/s^{-1} [11]. This value was considered too low to be important, especially for micro-molar (or lower) concentrations. Also, the reduction of Fe^{3+} back to Fe^{2+} is around 100 times slower. However, at near-neutral pH, Fe^{3+} in aqua- hydroxy- complexes is often found with lower reduction potentials [199], due to its coordination by the hydroxide anion (OH^-). The result is a reaction constant k around 20.000-30.000 M^{-1} s^{-1}, which withholds more implications; this high reactivity indicates the need for the bacteria to scavenge the intracellular nano-quantities of H_2O_2, because of the apparent toxic activity implicated [162].

4.1.2. Light-assisted H_2O_2 mode of action

In general, H_2O_2 addition is performed in μM to mM range, which places the action into the Mode I killing, because the concentrations used might be considered as low; Rincon and Pulgarin, Spuhler et al., or Garcia-Fernandez et al. [31,40,204] below 15 mg/L (0.44 mM) did not find any inactivation, Sciacca et al. with 10 mg/L (0.29 mM) found 2-log reduction and Ndounla et al. negligible inactivation in the dark with 8.5 mg/L (0.25 mM) H_2O_2 [30,45]. Nevertheless, the diffusion into the cell, and the light addition into the sample can offer conditions for effective internal photo-Fenton reaction and fast regeneration of ferric iron back to ferrous.

The first instance of synergistic inactivation by near-UV light and H_2O_2 was demonstrated by Anathaswamy and Eisenstark [205] for phages and Hartman and Eisenstark some years later [206] for *E. coli* K-12. The following years many works have been developed to assess the H_2O_2-enhanced photokilling modes and parameters that are involved [30,31,40,207–212]. The majority of the works agree that the involved mechanism is in fact a light-enhanced internal photo-Fenton reaction. The prevailing mechanism is as follows.

1) The direct damage of the light affects the DNA and the enzymes responsible for its reparation (direct action).
2) Light is disrupting the normal ROS-scavenging enzymes into the cells such as catalase, superoxide dismutase, peroxidases etc. (indirect action).
3) H_2O_2 penetrates the cell, causing imbalance of ROS into the cells.
4) ROS and light release iron into the cytoplasm, with reacts with H_2O_2 to create $HO^{\bullet}$. Other ROS are involved into the reduction of iron, or directly attack susceptible moieties (oxidative stress).
5) Added H_2O_2 affects bacterial membrane (outer damage), initiating its auto-oxidation.
6) Light reduces ferric iron to ferrous directly, through ligand-to-metal charge transfer (LMCT) or indirectly, through the reactive intermediates available by the light-induced malfunctioning into the cell, initiating a photo-catalytic cycle.

Concerning the suggested mechanism, there are some indications that confirm the majority of these actions or limit them to a certain extent. For instance, it is suggested that in aerobic, near-neutral conditions, the LMCT could not proceed for hours [213], so the sources of iron need to be replenished. In the majority of the cases, this time frame will not be required for bacterial inactivation; nevertheless, in these conditions Fe^{3+} is expected to precipitate and not participate further into the inactivation mechanism. Also, there was a linear increase of the inactivation kinetics by increasing the added H_2O_2 from 0 to 500 mM or 0 to 10 mg/L for Fisher et al. or Garcia-Fernandez et al. [40,207], respectively. It is suggested that the internal Fenton is taking place and also, Fe^{2+} is not the limiting reagent in the reaction. Therefore, there is a constant iron release and reduction, in an efficient catalytic cycle.

4.2. Addition of iron (Fe^{2+}/Fe^{3+})

So far, the light-induced oxidative stress and the voluntary addition of H_2O_2 have been assessed. In these actions, one has direct or indirect internal damage by light, and establish an internal photo-Fenton process. H_2O_2 addition has proven to enhance the internal photo-Fenton, therefore in this part, we present the events that take place if the matrix contains iron or if iron is added at will. The various events, such as the homogeneous Fenton, the heterogeneous Fenton and the semiconductor mode of action by the iron oxides will be further analyzed. But first, the role of iron, and its various forms in natural waters are presented.

4.2.1. Iron as the Fenton reaction catalyst

More than 100 years after the discovery of the Fenton reaction, iron still remains the most commonly employed metal catalyst for the fulfillment of $HO^{\bullet}$ generation with this method [214]. The use of iron entails a series of characteristics which are rarely encountered simultaneously in other metals. For instance, its versatility in gaining various oxidation states (−2 to +6), which derives from its position in the periodic table of elements [215], the characteristic abundance as far as its mass availability is concerned, the low toxicity implicated in its utilization and easy integration, state iron as the principal facilitator of the Fenton reaction [214]. Its coexistence with H_2O_2 initiates the Fenton reaction. The different types of Fenton reaction are summarized in Table 2 [216].

The most common forms of iron salts used for the Fenton reaction is Fe^{2+} and Fe^{3+}. These two salts are used mostly due to the low mass transfer limitations among them and the oxidants [217]. Fe^{2+} is always observed to be more effective than Fe^{3+} as a starting form of iron in the process. One of the main differences among the two forms are the characteristic insolubility of Fe^{3+} in slightly acidic and near-neutral pH values, making it difficult to operate outside the strict acidic region [215]. pH dependence is a matter strongly affecting iron speciation, and will be further analyzed later. Also, although Fe^{2+} is borderline categorized as a hard acid, Fe^{3+} shows a preference in hard oxygen ligands; Fe^{2+} favors sulfur and nitrogen

Table 2
The different types of the Fenton reaction (adapted from [218]).

Process	Reagents	Light	pH	Iron Loss
Classic Fenton	H_2O_2, Fe^{2+}	No	2–4	Yes
Fenton-like	H_2O_2, Fe^{3+}	No	2–4	Yes
Photo-Fenton	H_2O_2, iron complexes, free iron ions	Yes	Acidic to neutral	Yes
Heterogeneous Fenton	H_2O_2, solid iron oxide	No	wide range	No
Heterogeneous photo-Fenton	H_2O_2, solid iron oxide	Yes	wide range	No

Table 3
Proposed reaction mechanism for the Fenton (-like) reaction with H_2O_2 (25 °C and I = 0.1 M) (adapted from [220]).

Reaction No.	Reaction	Reaction Constant
(1)	$Fe^{3+} + H_2O \leftrightarrow Fe(OH)^{2+} + H^+$	$(k_1 = 2.9 \times 10^{-3} M)$
(2)	$Fe^{3+} + 2H_2O \leftrightarrow Fe(OH)_2^+ + 2H^+$	$(k_2 = 7.62 \times 10^{-7} M^2)$
(3)	$2Fe^{3+} + 2H_2O \leftrightarrow Fe_2(OH)_2^{4+} + 2H^+$	$(k_{2.2} = 0.8 \times 10^{-3} M)$
(4)	$Fe^{3+} + H_2O_2 \leftrightarrow Fe^{3+}(HO_2)^{2+} + H^+$	$(kI_1 = 3.1 \times 10^{-3})$
(5)	$Fe(OH)^{2+} + H_2O_2 \leftrightarrow Fe^{3+}(OH)(HO_2)^+ + H^+$	$(kI_2 = 2 \times 10^{-4})$
(6a)	$Fe^{3+}(HO_2)^{2+} \rightarrow Fe^{2+} + HO_2^{\bullet}$	$(k_6 = \times 10^{-3} s^{-1})$
(6b)	$Fe^{3+}(OH)(HO_2)^+ \rightarrow Fe^{2+} + HO_2^{\bullet} + OH^-$	$(k_6 = \times 10^{-3} s^{-1})$
(7)	$Fe^{2+} + H_2O_2 \rightarrow Fe^{3+} + HO^{\bullet} + OH^-$	$(k_7 = 63 M^{-1} s^{-1})$
(8)	$Fe^{2+} + HO^{\bullet} \rightarrow Fe^{3+} + OH^-$	$(k_8 = 3.2 \times 10^8 M^{-1} s^{-1})$
(9)	$HO^{\bullet} + H_2O_2 \rightarrow HO_2^{\bullet} + H_2O$	$(k_9 = 3.3 \times 10^9 M^{-1} s^{-1})$
(10a)	$Fe^{2+} + HO_2^{\bullet} \rightarrow Fe^{3+}(HO_2)^{2+}$	$(k_{10a} = 1.2 \times 10^6 M^{-1} s^{-1})$
(10b)	$Fe^{2+} + O_2^{\bullet-} + H^+ \rightarrow Fe^{3+}(HO_2)^{2+}$	$(k_{10b} = 1 \times 10^7 M^{-1} s^{-1})$
(11a)	$Fe^{3+} + HO_2^{\bullet} \rightarrow Fe^{2+} + O_2 + H^+$	$(k_{11a} < 2 \times 10^3 M^{-1} s^{-1})$
(11b)	$Fe^{3+} + O_2^{\bullet-} \rightarrow Fe^{2+} + O_2$	$(k_{11b} = 5 \times 10^7 M^{-1} s^{-1})$
(12a)	$HO_2^{\bullet} \rightarrow O_2^{\bullet-} + H^+$	$(k_{12a} = 1.58 \times 10^5 M^{-1} s^{-1})$
(12b)	$O_2^{\bullet-} + H^+ \rightarrow HO_2^{\bullet}$	$(k_{12b} = 1 \times 10^{10} M^{-1} s^{-1})$
(13a)	$HO_2^{\bullet} + HO_2^{\bullet} \rightarrow H_2O_2 + O_2$	$(k_{13a} = 8.3 \times 10^5 M^{-1} s^{-1})$
(13b)	$HO_2^{\bullet} + O_2^{\bullet-} + H_2O \rightarrow H_2O_2 + O_2 + OH^-$	$(k_{13b} = 9.7 \times 10^7 M^{-1} s^{-1})$
(14a)	$HO^{\bullet} + HO_2^{\bullet} \rightarrow H_2O + O_2$	$(k_{14a} = 0.71 \times 10^{10} M^{-1} s^{-1})$
(14b)	$HO^{\bullet} + O_2^{\bullet-} \rightarrow O_2 + OH^-$	$(k_{14b} = 1.01 \times 10^{10} M^{-1} s^{-1})$
(15)	$HO^{\bullet} + HO^{\bullet} \rightarrow H_2O_2$	$(k_{15} = 5.2 \times 10^9 M^{-1} s^{-1})$

Table 4
Oxides and hydroxides comprehensive list (adapted from [228]).

Oxide Hydroxides		*Oxides*	
Name	Formula	Name	Formula
Goethite	α-FeOOH	Hematite	α-Fe_2O_3
Lepidocrocite	γ-FeOOH	Magnetite	Fe_3O_4 ($Fe^{II}Fe_2^{III}O_4$)
Akaganéite	β-FeOOH	Maghemite	γ- Fe_2O_3
Schwertmannite	$Fe_{16}O_{16}(OH)_y(SO_4)_z \cdot nH_2O$		β- Fe_2O_3
	δ-FeOOH		ε- Fe_2O_3
Feroxyhite	δ'-FeOOH	*Wüstite*	FeO
High pressure	FeOOH		
Ferrihydrite	$Fe_5HO_8 \cdot 4H_2O$		
Bernalite	$Fe(OH)_3$		
	$Fe(OH)_2$		
Green rusts	$Fe_x^{III}Fe_y^{II}(OH)_{3x+2y-z}(A^-)_z$		

ligands [215]. Finally, among the Fenton reactions initiated by Fe^{2+} or Fe^{3+}, a small differentiation has been made, and if the starting form of iron is Fe^{3+}, the reaction is named Fenton like. A summary of the Fenton and Fenton-like reactions is proposed in Table 3.

A summary of the main parameters which affect the oxidation of Fe^{2+} to Fe^{3+}, is given in the following equation [219]:

$$\frac{d\left[Fe^{2+}\right]}{dt} = k\left[OH^-\right]^2 P_{O_2}\left[Fe^{2+}\right] \quad \text{(III.1)}$$

Where the pH (represented by OH^-), partial pressure of oxygen and initial Fe^{2+} concentration are the actors which influence the kinetics of the reaction. As it appears, pH is the most influencing factor in the rates of iron oxidation, and has to be analyzed separately.

4.2.2. Influence of the matrix pH

Theoretically, Fe^{2+} drives the homogeneous Fenton reaction. However, Morgan and Lahav [152] have analyzed the importance of pH in the distribution of iron species in the solution. Fe^{2+} forms hydroxide species, which have varying solubility rates in water, depending on the pH. The rate of oxidation and different species are included in the following equation, which accounts for the various soluble iron species.

$$-\frac{d\left[Fe^{2+}\right]}{dt} = \left(k_0\left[Fe^{2+}\right] + k_1\left[Fe(OH)^+\right] + k_2\left[Fe(OH)^0_{2(aq)}\right] + k_3\left[Fe(OH)_3^-\right]\right) DO, \quad \text{(III.2)}$$

Where partial pressure is replaced by dissolved oxygen, since this is participating in the oxidation reaction, and k_1, k_2, k_3 are oxidation rate constants.

The main regions of interest, as far as Eq. (2) is concerned, are below 4, between 5 and 8 and above 8. At pH < 4, Fe^{2+} is the main species. Between 5 and 8, $Fe(OH)^0_{2(aq)}$ concentration is pH-dependent (increasing from 5 to 8) and above 8, it is the dominating form. According to [152], the three species in Eq. (III. 2) have presented first order rate constants of $k_0 = 6 \times 10^{-5}$, $k_1 = 1.7$, and $k_2 = 4.3 \times 10^{+5}$ min^{-1}, which is a big difference and also indicates the main Fe-species in near-neutral pH. Below a pH value of 10, $Fe(OH)_3^-$ is not likely to affect the process, since its concentration is insignificant. Also, the necessary time to oxidize Fe^{2+} depending on the pH varies approximately from 50 min at pH = 7 to 175 at pH = 6.3 and very low, pH-independent at pH = 4 [152].

Considering the main Fenton reaction of Fe^{2+} with H_2O_2, we get:

$$Fe^{2+} + H_2O_2 \rightarrow \left[Fe^{3+} - OH\right] + HO^{\bullet} \quad \text{(III.3)}$$

According to the iron speciation diagram [214], at near-neutral pH $Fe(OH)_3$ and $Fe(OH)^+_2$ will be the predominant species. Fe^{3+} may form oxide and or precipitate on existing oxides [220]. However the question of iron oxides will be analytically presented in the

next chapter. The oxidized iron, will lead the heterogeneous Fenton reaction, either in the form of ferric hydroxides or as iron oxides.

At neutral pH, ferryl ion and $HO^{\bullet}$ compete on their formation from Fe^{2+}, as alternatives from the previous equation [221–223], reducing the efficiency of $HO^{\bullet}$ production, as ferryl is a less reactive species. Ultimately, the ferric species formed will create aqua hydroxy complexes [224]:

$$[Fe(H_2O)_6]^{3+} + H_2O \leftrightarrow [Fe(OH)(H_2O)_5]^{2+} + H_3O^{+} \quad \text{(III.4)}$$

$$[Fe(OH)(H_2O)_5]^{2+} + H_2O \leftrightarrow [Fe(OH)_2(H_2O)_4] + H_3O^{+} \quad \text{(III.5)}$$

And at near-neutral pH, we get [225]:

$$2[Fe(OH)(H_2O)_5]^{2+} \leftrightarrow [Fe_2(OH)_2(H_2O)_8]^{4+} + 2H_2O \quad \text{(III.6)}$$

$$[Fe_2(OH)_2(H_2O)_8]^{4+} + H_2O \leftrightarrow [Fe_2(OH)_3(H_2O)_7]^{3+} + H_3O^{+} \quad \text{(III.7)}$$

$$[Fe_2(OH)_3(H_2O)_7]^{3+} + [Fe(OH)(H_2O)_5]^{2+} \leftrightarrow [Fe_3(OH)_4(H_2O)_5]^{5+} + 7H_2O \quad \text{(III.8)}$$

4.2.3. Iron oxides: formation and basic properties

Iron oxides are the final product of iron transformation in nature. In total, 16 known oxides and hydroxides exist [226], presented in Table 4, and a range among them has been used in heterogeneous catalysis processes, recently reviewed by Pouran et al. [217]. As the ferrous state of iron is highly prone to oxidation, oxides are a deterministic product of the evolution through time. Also, oxides derive from ferric iron as well. Therefore, there are Fe^{2+} and Fe^{3+}-containing iron oxides, such as wüstite and goethite, respectively [216]. Jolivet et al. for instance have summarized the composition in $Fe^{2+}/^{3+}$ and hydroxylation ratio among the various iron oxides, indicating the existence of oxides with Fe^{2+} and Fe^{3+} in their composition [227].

The different hydroxides can be formed according to the conditions present in the matrix; for instance for pH > 3 hydroxylation of ferric ions can lead to ferrihydrite and hematite [227], or ferrous sulfate in water has led to lepidocrocite and goethite [59]. A comprehensive list of the possible iron (Fe^{2+} or Fe^{3+}) to iron oxides can be found in Fig. 6 [226]. Nevertheless, the significant/relevant interconversions are the ones taking place in natural water, *i.e.* slightly acidic or basic conditions, presence of organic matter, response to light, ambient temperature etc. The initial conditions of the oxides formation on the other hand could lead in the appearance of various forms of oxides in more special contexts; for instance mines or volcanic soils, where temperatures and pressure could lead to transformations and subsequently, transfer of the oxides to surface waters.

Oxide solubility in water varies and depends on the composition of the matrix, as well as the properties of the oxide itself [228]. More specifically, the presence or absence of ligand, and the ionic strength, as well as the pH of the solution (Table 5).

Table 6 [229] summarizes the pH for the zero point charge of the various oxides. This property is significant, as in natural water with the corresponding pH values present, their contact with microorganisms could be either favored or prevented. Another relevant property, for their participation in the Fenton reaction is the crystallinity. This property is a good indicator of potential release of iron into the bulk and subsequent utilization in the homogeneous Fenton (-like) reaction. For instance, Ferrihydrite and Schwertmannite have low crystalline properties and they are expected to release

Table 5
Interconversion among the iron oxides (adapted from [228]).

Precursor	Product	Type of Transformation	Preferred medium
Goethite	Hematite	Thermal or mechanical dehydroxylation	Gas/Vacuum
	Hematite	Hydrothermal dehydroxylation	Solution
	Maghemite	Thermal dehydroxylation	Air + Organic
Lepidocrocite	Maghemite/ Hematite	Thermal dehydroxylation	Gas/Vacuum
	Goethite	Dissolution/re-Precipitation	Alkaline Solution
	Magnetite	Reduction	Alkaline Solution with Fe^{2+}
Akaganéite	Hematite	Thermal dehydroxylation	Gas/Vacuum
	Goethite	Dissolution/re-Precipitation	Alkaline Solution
	Hematite	Dissolution/re-Precipitation	Acid Solution
	Magnetite	Dissolution/Reduction	Alkaline Solution with N_2H_4
δ-FeOOH	Hematite	Thermal dehydroxylation	Gas/Vacuum
Feroxyhyte	Goethite	Dissolution/re-Precipitation	Alkaline Solution
Ferrihydrite	Maghemite /Hematite	Thermal Dehydration/Dehydroxylation	Gas/Vacuum
	Goethite	Dissolution/re-Precipitation	Aqueous Solution pH 3–14
	Akaganéite	Dissolution/re-Precipitation	Acidic Media + Cl
	Lepidocrocite	Dissolution/re-Precipitation	pH = 6 + cysteine
	Hematite	Aggregation	Aqueous Solution pH 6–8
	Hematite	Short-Range Crystallization with Ferrihydrite	Aqueous Solution pH 6–8
	Substituted Magnetite	Dissolution/re-Precipitation	Alkaline Solution + M^{II}
Hematite	Magnetite	Reduction	Reducing gas
	Magnetite	Reduction-Dissolution/re-Precipitation	Alkaline Solution with N_2H_4
Magnetite	Maghemite/ Hematite	Oxidation	Air
Maghemite	Hematite	Thermal Conversion	Air
$Fe(OH)_2$	Magnetite	Oxidation	N_2 + alkaline solution
	Goethite		Alkaline Solution
	Lepidocrocite		
	Magnetite		
	Maghemite		
FeO	Magnetite + Fe	Disproportionation	Air

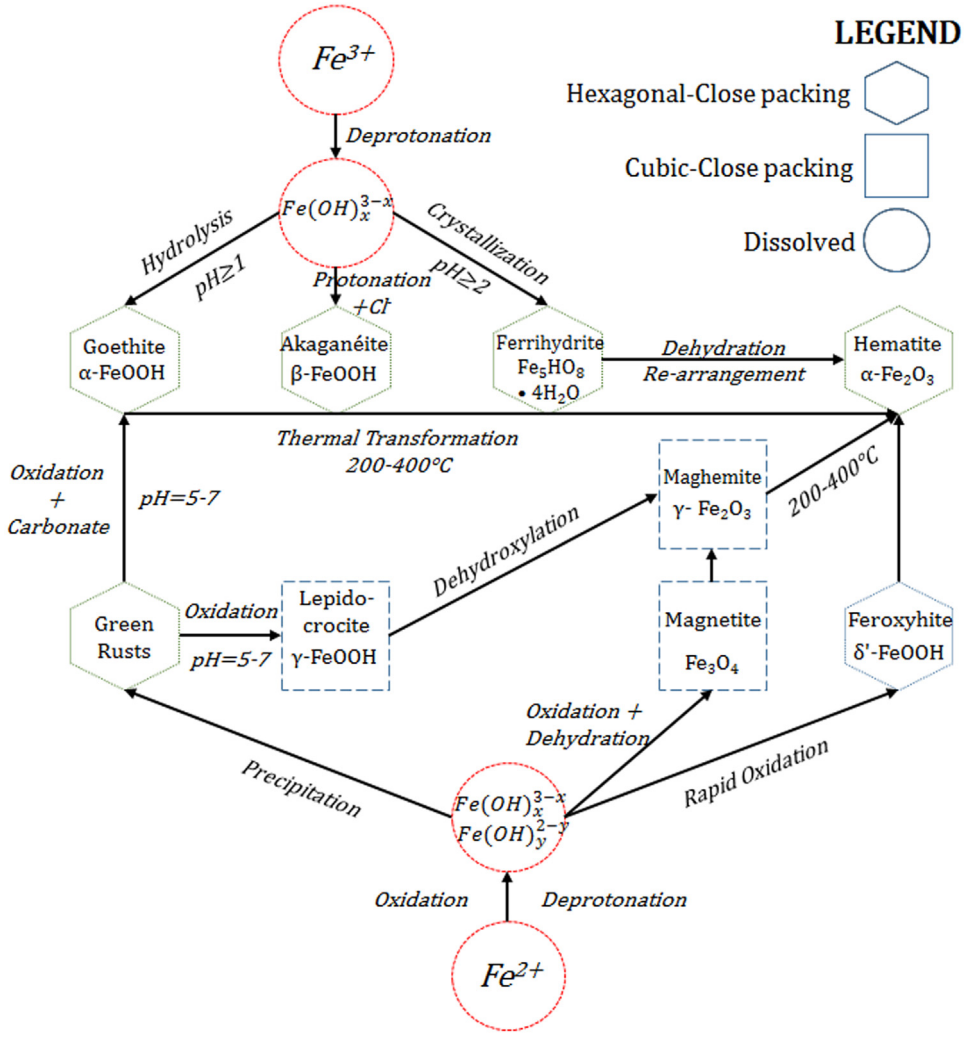

Fig. 6. Iron oxides formation and transformation (adapted from [226]). The different pathways of oxides transformation are presented, including both the ones taking place in natural waters, as well as the (theoretically) potentially present due to previous terrestrial properties.

more iron ions than oxides with similar content but high crystallinity [216].

Finally, of particularly high interest are the oxides which have oxidizing or good photochemical properties, like α-Fe_2O_3, γ- Fe_2O_3, α-Fe-OOH, β-FeOOH and γ-FeOOH. These oxides will be expected to contribute in the photo-enhanced Fenton reaction in near-neutral media [230,231], actively participating either as sources of homogenous iron, heterogeneous catalysts or semiconductors.

4.2.4. Iron, light supply and bacterial presence facilitate the photo-Fenton reaction

Before the simultaneous presence of iron and H_2O_2 is further analyzed, the sole addition of iron will follow, as it can have bactericidal properties by itself. After the initial oxidation of Fe^{2+}, the next steps of the process involve Fe^{3+}-initiated reactions. Fe^{3+} is thermodynamically more stable than Fe^{2+}, but is also less soluble [232]. Even at near-neutral pH, this is not a detrimental constraint, since Fe^{3+} can be reduced back to Fe^{2+} by different mechanisms. First of all, it must be noted that the reduction process is in competition with precipitation. Since the iron-containing solids have big specific surface area [233] they can complex with ligands, or react with oxidants/reductants; electron transfer is then facilitated. Therefore, the possible routes back to Fe^{2+}, involve reduction of i) organically or inorganically complexed iron, ii) dissolved inorganic

Table 6
pH and isoelectric points of the various iron oxides (adapted from [231]).

Sample	pH (point zero charge)
Fe^0	7.8–8.1
Fe_3O_4	6.3–8.72
α-Fe_2O_3	5.2–8.96
γ-Fe_2O_3	8.25
α-FeOOH	7–9.5
β-FeOOH	6.5–6.9
γ-FeOOH	7.05–8.47
δ-FeOOH	8.5
$Fe_5HO_8{\cdot}4H_2O$	8.9

Fe^{3+}, iii) microorganism-complexed iron and iv) matrix-assisted (*i.e.* thermal, abiotic) processes [234–240]. After its conversion back to Fe^{2+}, even in small amounts, electron transfer is very fast, and iron is established as an efficient catalyst and a considerable electron source [233].

4.2.4.1. Complexed iron: organic, aqua- and aqua-hydroxy-complexes. In principle, the available complexes are encountered in water through multiple routes, including precipitation, exchange with soils and urban activities [241–248]. One option is the carboxylate group ($R\text{-}COO^-$) which facilitates iron complexation. The polycarboxylates facilitate the photo-Fenton reaction, as they are

photo-active under solar light, and initiate a number of Fenton-related actions. Before we analyze the mechanism of reduction, we mention that some of the products of photo-reduction include the superoxide/hydroperoxide radical ($O_2^{\bullet-}/HO_2^{\bullet-}$) and H_2O_2 [241,249]; the photo-Fenton reaction is again initiated by Fe^{2+} and H_2O_2, and $HO^{\bullet}$ is produced anew.

There are two mechanisms of iron regeneration under light, *via* either an inner or an outer electron transfer mechanism [250]. Firstly, the [Fe^{3+}-L_n] is excited to [Fe^{3+}-L_n]* state, and i) *via* the inner-sphere mechanism $L^{\bullet+}$ is formed, and [Fe^{2+}-L_{n-1}]. In reaction with another ligand and oxygen, the parent [Fe^{3+}-L_n] is regenerated or ii) *via* an electron donor (which gets oxidized) and the reaction of [Fe^{2+}-L_n] with molecular oxygen [250]. In both cases, a sacrificial electron donor is required and superoxide anion is formed, which, as analyzed before, has its own biological significance. Solar light is energetic enough to overpass the ligand-to-metal charge transfer (LMCT) band only if the organic ligand is easily oxidized; in natural waters this is easy to get and therefore, this reaction is deeply meaningful.

The one-electron oxidation of the bidentate ligand generated within the process requires a second electron transfer to return to stable oxidation states, by the following reaction scheme:

$$\left[Fe^{+3}-L\right]^{3+}+2H_2O\overset{h\nu(LMCT)}{\rightarrow}[Fe(H_2O)_2]^{2+}+L^{\bullet+} \quad \text{(III.9)}$$

$$L^{\bullet+}+\left[Fe^{+3}-L\right]^{3+}\rightarrow[Fe^{2+}-L]^{2+}+L^{2+} \quad \text{(III.10)}$$

$$L^{\bullet+}+O_2\rightarrow L^{2+}+O_2^{\bullet-} \quad \text{(III.11)}$$

$$L^{\bullet+}+Cu^{2+}\rightarrow L^{2+}+Cu^{+} \quad \text{(III.12)}$$

The oxidized ligand can react either by a) with the parent Fe^{3+}-L complex, b) with oxygen, creating superoxide radical anion or c) with other oxidants in the matrix [250,251]. The unstable superoxide radical anion is leading to H_2O_2 formation or biological damage; it is therefore made clear that the photo-Fenton cycle by-products initiate more pathways towards bacterial inactivation.

Within the aqua- hydroxy complexes, there is a limited availability in neutral pH. [$Fe^{3+}OH(H_2O)_5$] is one of the remaining complexes in slightly acidic environments, which is photoactive [252]. In the case of aqua and/or aqua hydroxy complexes, the main difference lies in the ligand oxidation product, which in this case is $HO^{\bullet}$ [253]. Therefore, in near neutral pH, inner sphere LMCT can take place and transfer electron to Fe^{3+}, to generate Fe^{2+} and $HO^{\bullet}$:

$$[Fe^{3+}(OH)(H_2O)_5]^{2+}+H_2O\overset{h\nu(LMCT)}{\rightarrow}[Fe^{2+}(H_2O)_6]^{2+}+HO^{\bullet} \quad \text{(III.13)}$$

In other Fe-hydroxo complexes, there are similar pathways [230,240], which can be summarized as:

$$\left[Fe^{3+}OH(H_2O)_5\right]+H_2O\overset{h\nu(LMCT)}{\rightarrow}\left[Fe^{2+}(H_2O)_6\right]+HO^{\bullet} \quad \text{(III.14)}$$

$$\left[Fe^{2+}(H_2O)_6\right]+OH^{-}+O_2\rightarrow\left[Fe^{3+}OH(H_2O)_6\right]+H_2O \quad \text{(III.15)}$$

Among the two categories of ligands, only around 10–20% is waterbound, with the most abundant species, being the organically-complexed iron forms [254,255].

4.2.4.2. Iron-microorganism interaction. Iron holds the property of binding to surfaces which can provide the necessary electrostatic conditions. In the previous chapters, the chelating properties of organic ligands were presented together with the water-iron complexes, as well as the iron inter-conversion in these cases. Although microorganisms are far more complex entities than organic compounds, there are some noteworthy properties that influence iron, such as: i) the overall solubility of iron in the matrix and ii) the iron formation within it.

Bacterial membranes consist in layers, which, on the outer surface, contain lipo-polysaccharide molecules (LPS). These LPS have been documented to bind bivalent molecules [256], and therefore offer binding sites to iron as well. The second macro-observation is that Fe^{3+} can form complexes with big macromolecules, which could mean that iron-bacteria aggregates can be formed [257]. As it is made clear, Fe^{2+} after its oxidation to Fe^{3+} can remain in suspension (even for a short period) and use the bacterial membrane as a ligand. Therefore, LMCT can occur, among the iron and the surface binding it [31]. As a result, reduction of Fe^{3+} takes place and the oxidation of the ligand, as it was described before, damages the external bacterial surface [50].

Even in absence of light, there were important observations of groups studying the iron oxides' interaction with bacteria [217,258,259], where different strains of both Gram negative or positive bacteria were found to be partially, up to fully covered in iron oxides. This could initiate a strong oxidative damage on the bacterial surface if the proper conditions are met. Also, another set of observations led to the influence of iron form if bacteria were present in a sample. It was shown [259] that letting the microorganisms age in a sample and allow the subsequent release of proteins and DNA (from dead cells) influenced the formation of specific iron oxide structures. As it appears, the iron oxides' formation is affected also by the presence of microorganisms, in a process called "oriented aggregation" [260,261] apart from the pH, temperature and oxygen constraints mentioned before.

4.2.5. Homogeneous and heterogeneous Fenton, photo-Fenton and semiconductor action mode, during simultaneous presence of hν, H_2O_2 and Fe

Continuing from the enhancement by H_2O_2, we assume now that iron is inserted into the photo-inactivation process. Fe^{2+} was described in a previous chapter and the presence of oxygen, in combination with pH were defined as the combined oxidation triggers. In a similar system, hydrogen peroxide can also determine the oxidation rate [262], converting Fe^{2+} to Fe^{3+}. The ferrous ion is considerably more soluble, is readily oxidizable or assimilable by bacteria [263], but has lower complexing capabilities than Fe^{3+}; considering the oxidative conditions present, it is not expected to remain long in this valence [262] (Fig. 7).

Nevertheless, the first step of the Fenton reaction is taking place efficiently, with simultaneous generation of Fe^{3+} and $HO^{\bullet}$. In this part, we will attempt to concentrate the different photo-catalytic actions involved by the simultaneous addition of Fe salts and H_2O_2 and synthesize the inactivation mechanism dominating bacterial inactivation.

4.2.5.1. Step 1: addition of Fe^{2+} → internal action. Fe^{2+} in absence of H_2O_2 in the water matrix, has limited reactivity. However, it can diffuse into the bacterial cell quite easily [148,153] due to low charge density and difference in osmotic pressure between the cell and the matrix. From this point and onwards, it is available as a readily oxidizable catalyst, able to induce oxidative stress internally with the H_2O_2 produced as a normal part of the respiration chain. Considering an illuminated system, which, as we have analyzed, affects the regulation of ROS into the cell, the reaction with H_2O_2 becomes a photo-catalytic process; Fe^{3+} binds in various positions and uses a LMCT to regenerate back to Fe^{2+}, or $O_2^{\bullet-}$ and induces a constant release of Fe from the Fe/S clusters in the cell.

$$Fe^{2+}+H_2O_2\rightarrow Fe^{3+}+HO^{\bullet}+OH^{-} \quad \text{(III.16)}$$

$$Fe^{3+}+H_2O_2\rightarrow Fe^{2+}+HO_2^{\bullet}+H^{+} \quad \text{(III.17)}$$

$$Fe(OH)^{2+}+h\nu\rightarrow Fe^{2+}+HO^{\bullet} \quad \text{(III.18)}$$

$$[Fe(COO-R)]^{2+}+h\nu\rightarrow Fe^{2+}+CO_2+R^{\bullet} \quad \text{(III.19)}$$

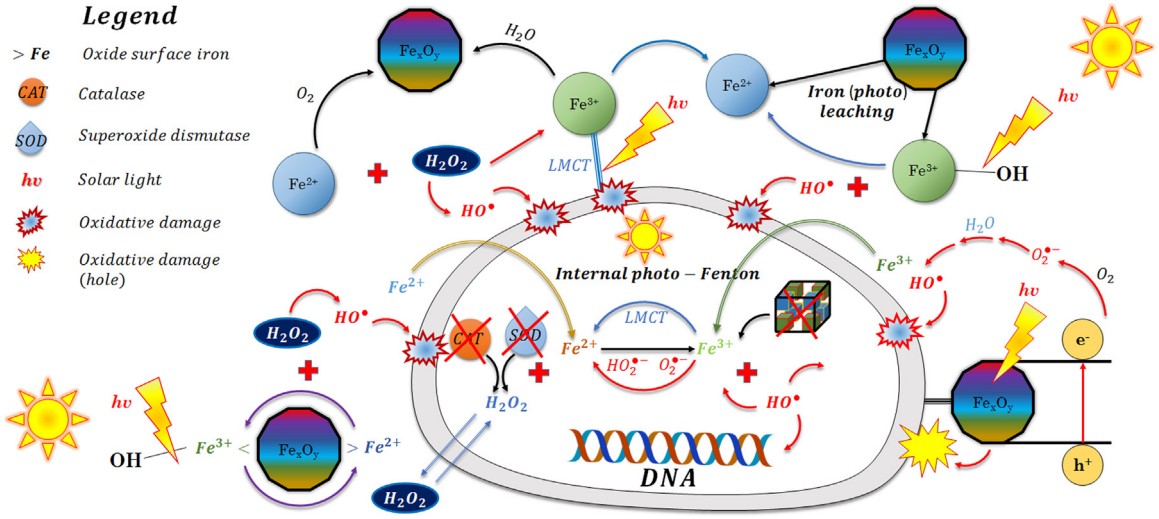

Fig. 7. Summary of the contribution by Fe and H_2O_2 enhancements. The analytical explanations of the various actions are analyzed in-text, at steps 1–6.

This process has been proven of significance [31,50]. The internal process has been found to be important, when the internal and the external damage were compared through malondialdehyde (MDA) formation [50]. Both in bacteria [264] and in another microorganism (*Saccharomyces cerevisiae*) it was proven through proteomic analyses that internal photo-Fenton is the main driving force of inactivation [71].

4.2.5.2. Step 2: addition of Fe^{2+} → external action (including chelating agents). Fe^{2+} addition, in presence of H_2O_2 in the matrix, can drive a homogeneous photo-Fenton process, for a limited period of time. Fe^{2+} is soluble in water, and by reaction with H_2O_2, production of $HO^{\bullet}$ is achieved in a big extent, effectively degrading the external cell membrane and resulting in microorganism degradation. However, we have analyzed the fate of Fe^{2+} in near-neutral pH and in presence of dissolved oxygen and/or H_2O_2; Fe^{3+} is expected to be formed, which in turn has limited dissolution rates in these conditions, except if it is complexed with organic ligands (its activity will be analyzed in step 3). In order to mitigate the problem of iron availability in unfavorable conditions, the use of chelating agents has been assessed for bacterial inactivation [68]. Fe^{2+} was provided by a stable (in the dark) Fe-citrate complex, whose light-initiated dissociation was as follows:

$$\left[Fe^{3+} - \text{citrate}\right] + h\nu \rightarrow Fe^{2+} + \text{citrate}^{2\bullet -} \quad \text{(III.20)}$$

$$\text{citrate}^{2\bullet -} + O_2 \rightarrow \textit{product} + CO_2 + O_2^{\bullet -} \quad \text{(III.21)}$$

$$Fe^{2+} + O_2 \rightarrow Fe(OH)^{2+} \rightarrow Fe(OH)_2^{+} \quad \text{(III.22)}$$

$$Fe^{3+} + O_2^{\bullet -} \rightarrow Fe^{2+} + O_2 \quad \text{(III.23)}$$

Under irradiation of the photo-active complexes (main form at near-neutral pH: [FeHcit], $[Fecit]^{-}$, $[Fecit]^{2-}$ and $[FeHcit]^{+}$, [Fecit], $[FeOHcit]^{-}$, for ferrous and ferric complexes, respectively) Fe^{2+} was released, according to the following reactions:

$$[Fe(OH) - \text{citrate}]^{-} + h\nu \overset{LMCT}{\rightarrow} Fe^{2+} + 3 - HGA^{2\bullet -} \quad \text{(III.24)}$$

$$\left[Fe^{2+} - \text{citrate}\right]^{-} + H_2O_2 \rightarrow \left[Fe^{3+} - \text{citrate}\right] + OH^{-} + HO^{\bullet} \quad \text{(III.25)}$$

$$HO_2^{\bullet} \leftrightarrow O_2^{\bullet -} + H^{+},\ pK_a = 4.8 \quad \text{(III.26)}$$

$$HO_2^{\bullet} + O_2^{\bullet -} + H_2O \rightarrow H_2O_2 + O_2 + OH^{-} \quad \text{(III.27)}$$

$$HO_2^{\bullet} + HO_2^{\bullet} \rightarrow H_2O_2 + O_2 \quad \text{(III.28)}$$

Due to the presence of the ligand, effective bacterial inactivation was obtained up to pH = 8.5, by production of $HO^{\bullet}$ and $O_2^{\bullet -}$, measured by electron spin resonance (ESR) spectroscopy. The citrate by-products, as the ligands in the LMCT presented in previous chapters, can react with molecular oxygen or H_2O_2 to initiate further ROS production, mainly superoxide radical anion [18].

4.2.5.3. Step 3: Fe^{3+} formation/addition (in presence of bacteria). Fe^{3+} has been shown to form after the oxidation of Fe^{2+}, inside and outside the cell. Into the cell, upon formation Fe^{3+} can bind to proteins and DNA backbone, efficiently participating in LMCT-initiated oxidative damage. Fe^{3+} can also play the role of electron acceptor during UV-affected dumping of electrons, during malfunctioning of the respiration process [31]. Furthermore, bacteria are known to produce siderophores such as enterobactin, aerobactin, and ferrichrome, which are able to metabolically chelate Fe^{3+} present in the cell [265,266], to cover their needs in Fe^{3+}. These proteins efficiently bind to Fe^{3+} and create complexes, therefore facilitating internal photo-assisted LMCT and production of $HO^{\bullet}$.

$$Fe^{3+} - \text{siderophore} + h\nu \overset{LMCT}{\rightarrow} Fe^{2+} + L^{\bullet +} \quad \text{(III.29)}$$

On the other hand, siderophores are not limited to internal activity, but, along with the bacterial membranes, can facilitate external iron availability, as follows: the reduced diffusion capability of Fe^{3+} is overpassed by transfer proteins, which bring Fe^{3+} into the cytoplasm. From this point it can play the aforementioned roles. Outside the cell, Fe^{3+} binds to the bacterial membrane possessing high affinity compounds, such as carboxylic groups [31] or phospholipids and lipo-polysaccharides [267] as described in the previous chapter, forming Fe-bacterium complexes or nFe^{3+}-mBacteria agglomerates. The photo-initiated electron transfer by LMCT creates local, external oxidative damage and the oxidized ligand could continue the oxidative chain reaction, producing more ROS. The production of Fe^{2+} from this process re-initiates steps 1 and 2.

4.2.5.4. Step 4: iron oxides formation from Fe^{2+}/Fe^{3+} addition. After conversion of Fe^{2+} to Fe^{3+}, the Fenton process is considered as limited, since $Fe(OH)^{2+}$ has limited solubility at near-neutral pH and therefore, exploitation of its photoactivity is limited [50]. Instead, zero-charge complexes are formed, such as $Fe(OH)_2^0$, which are prone to oxidation and formation of solid iron oxides, such as magnetite, goethite, lepidocrocite, or feroxyhyte [227]. Measurements have shown that iron precipitates as ferric oxide or hydroxide, often with formation of goethite and/or lepidocrocite (α-FeO(OH) and

γ-FeO(OH), respectively) [226]. This is why usually soluble iron precipitates after some time in Fenton experiments in near-neutral pH. As analyzed before, the formation of the oxides is affected by a number of parameters, and the different oxides could participate differently in the photo-catalytic inactivation mechanisms. The presence of H_2O_2 in the sample, as well as dissolved oxygen, normally initiates a series of reactions to create the oxides [59]:

$$Fe^{2+} + 6H_2O \rightarrow [Fe(H_2O)_6]^{2+}_{(aq)} \quad \text{(III.30)}$$

$$[Fe(H_2O)_6]^{2+}_{(aq)} + OH^- \rightarrow [Fe(OH)(H_2O)_5]^{+}_{(aq)} + H_2O \quad \text{(III.31)}$$

$$[Fe(OH)(H_2O)_5]^{+}_{(aq)} + OH^- \rightarrow [Fe(OH)_2(H_2O)_4]_{(aq)} + H_2O \quad \text{(III.32)}$$

$$Fe^{2+} + O_2 \rightarrow Fe^{3+} + O_2^{\bullet -} \quad \text{(III.33)}$$

$$Fe(OH)^+ + O_2 \rightarrow Fe(OH)^{2+} + O_2^{\bullet -} \quad \text{(III.34)}$$

$$Fe(OH)_2 + O_2 \rightarrow [Fe(OH)_2]^+ + O_2^{\bullet -} \quad \text{(III.35)}$$

$$4[Fe(OH)_2(H_2O)_4]_{(aq)} \rightarrow [Fe_4(OH)_8(H_2O)_8]_{(s)} + 8H_2O \quad \text{(III.36)}$$

$$[Fe_4(OH)_8(H_2O)_8]_{(s)} + O_2 \rightarrow 4FeOOH_{(s)} + 10H_2O \quad \text{(III.37)}$$

Furthermore, iron oxides, depending on their isoelectric point (IEP), can adsorb to bacterial surfaces [268,269]; oxides can be positively charged below the point of zero charge (ZPC), if the pH of the natural waters is $pH < pH_{PZC}$ [226], and their connection with bacterial membrane, being negatively charged between pH 3 and 9 [267], is permitted. In addition, Voelker et al. [270] have suggested also a small release of iron from the oxides. However, in presence of bacteria, some of the iron oxides are chelated either by siderophores, bacterial surfaces or bacterial degradation by-products. This increases the normally low solubility which these species present at neutral pH. Even more, their simultaneous availability with H_2O_2 and/or light initiates the next two mechanisms of inactivation, the semiconductor mode of action and the heterogeneous catalyst effect.

4.2.5.5. Step 5: semiconductor action mode of iron oxides. Iron oxides can function as either heterogeneous photo-catalysts or as semiconductors. The semiconductor action is not a step prior to the heterogeneous mechanism, but rather "a parallel" one. It will be presented first, as this pathway can evolve, even without H_2O_2 addition.

Iron oxides, either naturally present in water [226] or laboratory-prepared [226] are among the most reactive components within the matrix. Their chemical activity involves potential photocatalyst activity, if the hole-electron recombination (electron returning to an empty state) problem is overpassed [271]. The semiconductor action mode is described by the following equations [226] (the reactions taking place at the oxide surface are marked as $>Fe^{2+/3+}$):

$$Fe_2O_3 + h\nu \rightarrow Fe_2O_3\left(e^- + h^+\right) \quad \text{(III.38)}$$

$$e^-_{(cb)} + O_2 \rightarrow O_2^{\bullet -} \quad \text{(III.39)}$$

$$h^+_{(vb)} + O_2^{\bullet -} \rightarrow {}^1O_2 \quad \text{(III.40)}$$

$$e^-_{(cb)} + > Fe^{3+} \rightarrow > Fe^{2+} \quad \text{(III.41)}$$

$$h^+_{(vb)} + RX_{ad} \rightarrow RX^{\bullet +}_{ad} \quad \text{(III.42)}$$

$$e^-_{(cb)} + O_2^{\bullet -} + 2H^+ \rightarrow H_2O_2 \quad \text{(III.43)}$$

$$e^-_{(cb)} + H_2O_2 \rightarrow OH^- + HO^{\bullet} \quad \text{(III.44)}$$

Briefly, the mechanism involves the absorption of a photon with higher energy than the band gap, generating hole-electron pairs in the conduction and valence bands, respectively. Assuming that there is a fraction of efficient promotion, rather than 100% recombination, redox reaction can take place in the surface of the oxide [59]. Light is essential to initiate the reaction [226,272,273] creating the hole-electron pairs. The conduction band produces electrons, which can initiate superoxide radical anion production, with molecular oxygen as electron acceptor. Superoxide can either react with the holes to produce singlet oxygen, which has important biological significance, affect the external bacterial membrane themselves, or convert by-standing Fe^{3+} to Fe^{2+} [272,273]. The holes, on the other hand can create oxidative damage to the bacterial membranes themselves, since the positive oxidation potential of the holes (1.7 V at neutral pH), is under the redox potential of the outer layer of the bacterial membrane [273–276]. Another suggestion [273] proposes a scheme involving the production of $HO^{\bullet}$ and H_2O_2. If H_2O_2 is added in the bulk, then higher $HO^{\bullet}$ production is achieved, allowing more significant bacterial inactivation.

Ruales-Lonfat et al. [59] tested 4 iron oxides, 3 of which revealed a semiconductor mode of action, goethite, hematite and wüstite; magnetite failed to demonstrate such capabilities in absence of H_2O_2, possibly due to low band gap, unfavorable IEP, high agglomeration [277] or high precipitation dynamics of the Fe^{2+} content [278,279]. Nevertheless, it is significantly active under photo-Fenton conditions (with H_2O_2). In presence of bacteria, the siderophores affected the experiments, possibly by either enhancing dissolution of iron [266,280,281], electron transfer through LMCT in the Fe-siderophore complex, or a semiconductor-driven charge transfer of electron towards the oxide surface [281], leading to Fe^{3+} reduction.

4.2.5.6. Step 6: heterogeneous (photo) Fenton reaction. Iron oxides in presence of H_2O_2 can play the role of an efficient heterogeneous photo-catalyst, towards, bacterial inactivation [50,59], in two ways. Firstly, in presence of siderophores, they can contribute to the supply of dissolved Fe^{2+} in the bulk [266]. Furthermore, H_2O_2 can start a series of reactions, at which iron hydroxide ligands can get reduced, with simultaneous hydroperoxyl radical formation [266]. Under light, the production of hydroxyl radicals is also favored [282]. The reactions involved are the following:

$$> Fe^{3+} - OH + H_2O_2 \rightarrow > Fe^{2+} + HO_2^{\bullet} + H_2O \quad \text{(III.45)}$$

$$> Fe^{2+} + H_2O_2 \rightarrow > Fe^{3+} - OH + HO^{\bullet} + H_2O \quad \text{(III.46)}$$

$$> Fe^{3+} - OH + h\nu \rightarrow > Fe^{2+} + HO^{\bullet} \quad \text{(III.47)}$$

$$HO_2^{\bullet} \leftrightarrow O_2^{\bullet -} + H^+, \; pK_a = 4.8 \quad \text{(III.48)}$$

$$> Fe^{3+} - OH + HO_2^{\bullet}/O_2^{\bullet -} \rightarrow > Fe^{2+} + H_2O/OH^- + O_2 \quad \text{(III.49)}$$

As it is seems, even magnetite, which does not demonstrate semiconductor capabilities, was reported to efficiently inactivate *E. coli* when H_2O_2 was added in the bulk [59]. In step 5, the formation of quantities of H_2O_2 was also proposed, here we assess the possibility of H_2O_2 addition from the beginning; then the preferred pathway for the oxides would be to use H_2O_2 as electron acceptor (under light) or act as heterogeneous catalysts. The H_2O_2 accepting the electrons would further create $HO^{\bullet}$ radicals, and further regeneration of Fe^{3+} back to Fe^{2+} would be achieved.

An alternative mechanism includes the disruption of the excited $>Fe^{3+}OOH$ bond, resulting to $>Fe^{4+}=O$ species an $HO^{\bullet}$ d [283]. $>Fe^{4+}=O$ reacts with water and further produces $HO^{\bullet}$ radicals; a summary of the reaction scheme is as follows:

$$> Fe^{3+} - OH + H_2O_2 \rightarrow > Fe^{2+} + HO_2^{\bullet} + H_2O \quad \text{(III.45)}$$

$$> Fe^{3+} - OOH + h\nu \rightarrow > Fe^{4+} = O + HO^{\bullet} \quad \text{(III.50)}$$

$$> Fe^{4+} = O + H_2O \rightarrow > Fe^{3+} - OH + HO^{\bullet} \quad \text{(III.51)}$$

5. Chapter V: Influence of the water matrix

5.1. Influence of natural organic matter on the photo-Fenton reaction

The following conceptual part of this review assesses one of the most crucial components facilitating the near-neutral photo-Fenton in natural waters, the presence of natural organic matter (NOM). Its presence has been connected with both enhancement of the photo-Fenton reaction and partial hindering, under circumstances. In this chapter, the various forms, functions and effects of NOM will be presented.

5.1.1. Definitions—distinction among the components of NOM

Natural organic matter (NOM) is a general definition, bringing together all types of organic matter normally present in natural water bodies. The two major categories of NOM, are the dissolved organic matter (DOM) and the particulate organic matter (POM). The distinction among the two categories is facilitated through a convention set in the isolation technique, *i.e.* filtering with 0.1–0.7 μm diameter membranes [284]; DOM is the fraction that is passing through, while POM is retained [285]. A number of authors have proposed further distinction, from the permeate of ultrafiltration (< 10 kDaltons), being the real dissolved organic matter, and the fraction above 10 kDa and below 0.4 or 0.7 μm the "total dissolved organic carbon". The colloidal sizes are among 1 nm and 1 μm, with the dissolved fraction being a part of it [286–290].

DOM is the result of material run-off from soils, the algal or phytoplankton originated biological by-products in other surface waters, and the artificial, man-made substances that infiltrate natural waters; the three categories compose the allochthonous organic matter, varying from 10 to 300.000 kDa size [291–293]. However, there is a fraction of organic matter (OM) that is present and produced in the water body, the autochthonous part. Humic or fulvic substances, bacterial by-products, as well as organic acids, carbohydrates, proteins, lipids, alcohols, sterols, phenols and atmospheric organic matter are the rest of the major autochthonous fraction [285,294–299]. Finally, the particulate organic matter (POM) is by definition larger in size and is composed by floral debris, bacterial and higher microorganisms' by-products and is also often a function of the neighboring soil properties [284].

5.1.2. DOM functions in natural waters

The two main functions of DOM which facilitate its active participation in the photo-Fenton reaction are the photo-active behavior of certain moieties and its ability to complex metal cations, keeping them in solution and subsequently allowing their participation in homogeneous oxido-reductive cycles, without suffering high degree of precipitation.

5.1.2.1. Photo-activity: chromophoric and colored DOM. In general, DOM is reported to absorb light in both the UV and visible regions [285,296,299–302]. The fundamental difference among colored and chromophoric DOM (CDOM) is the absorption in the visible region. The substances absorbing in the visible region are denoted as colored. Among the NOM, a differentiation could be made among the high and low molecular weight DOM constituents (HMW and LMW DOM). HMW DOM absorbs in a range of 250–800 nm and more specifically, it includes the allochthonous fulvic and humic acids and the autocthnonous fulvic acids. The aforementioned substances are colored and can be marked as both colored and chromophoric DOM [284,299,303–307]. On the contrary, LMW DOM constituents absorb almost exclusively in the UV region and lack color. In detail, Mostofa et al. [284] have reviewed various components of the LMW DOM, such as formaldehyde, acetate, malonate and more, which absorb in 207–250 nm, 204–270 nm and 225–240 nm, respectively. These substances are classified as chromophoric DOM, but not colored DOM.

5.1.2.2. Complexation with trace metal ions. The ability of DOM to complex metal ions is of critical importance in making metals available in the environment. This ability is exploited also by the natural cycle of photo-Fenton, further analyzed later. Complexation is an indirect regulator of the overall chemistry of metal ions, affecting functions such as transport, acid-base balance, solubility in water and more [284]. Among the DOM constituents, many can participate in these functions, from both the allochthonous and autochthonous fractions. More specifically, humic and fulvic substances, amino acids, extracellular polymeric substances produced by bacteria have demonstrated complexing capabilities [308,309]. The diversity of the functional groups realize the complexation, with chromophoric and fluorophoric groups being among the most probable facilitators [285,310–312]. Finally, the most important measure of the DOM-metal interaction is the conditional stability constant. This parameter has been reviewed by Mostofa et al. [284] and the most important parameters have been found to be the size (and origin) of DOM, the matrix pH, the cations and anions present, the photochemical processes potentially involved and the contribution of microbial species. Since this constant is a function of a set of parameters, its value is expected to differ significantly.

5.1.3. DOM photo-chemistry and the Fenton reaction

The interaction between DOM and light has been repeatedly reported to generate ROS in natural waters. Highly reactive ROS, such as the hydroxyl radical ($HO^{\bullet}$) or less reactive/more selective, such as the superoxide radical anion ($O_2^{\bullet-}$), hydrogen peroxide (H_2O_2), singlet oxygen ($^1O_2$), are generated in-situ, when DOM is irradiated. In this chapter, the generation of ROS, the implicated photo-chemistry and the dual role of DOM will be analyzed further.

Fig. 8 summarizes the events that take place in natural waters, where the simultaneous presence of Fe, H_2O_2 and DOM is expected. Measurements have indicated their co-existence in natural waters in USA [313–315], therefore in the case of solar irradiation, once again an in-situ photo-Fenton reaction is initiated. Adding iron and H_2O_2 will only enhance the photo-Fenton already taking place, aggravating the oxidative stress for the microorganisms present in water. The different events (1–14) are analyzed below:

5.1.3.1. Event 1: contribution of particulate organic matter (POM). Particulate organic matter has been identified to contribute in the overall photochemistry, producing singlet oxygen [316] but it is also an indirect source of DOM for the bulk [317–321]. Therefore, it can be considered as input of DOM for the subsequent steps.

5.1.3.2. Event 2: direct photo-reactions of DOM with sunlight. In presence of organic matter, solar light is absorbed by DOM in the ground state and the excited singlet state is generated, leading to the conversion to the triplet state as explained in a previous chapter ($^3DOM^*$) [322,323]. The triplet state is an unstable form and will quickly react with molecular oxygen [324–328], producing singlet oxygen ($^1O_2$):

$$DOM + h\nu \rightarrow {}^1DOM \rightarrow {}^3DOM^* \quad \text{(IV.1)}$$

$$^3DOM^* + O_2 \rightarrow DOM + {}^1O_2 \quad \text{(IV.2)}$$

The termination of this reaction is reached with the return of DOM to its ground state. The singlet oxygen on the other hand will continue reacting (*i.e.* attacking bacteria), according to the schemes suggested in the previous chapters, or produce superoxide radical anions [329].

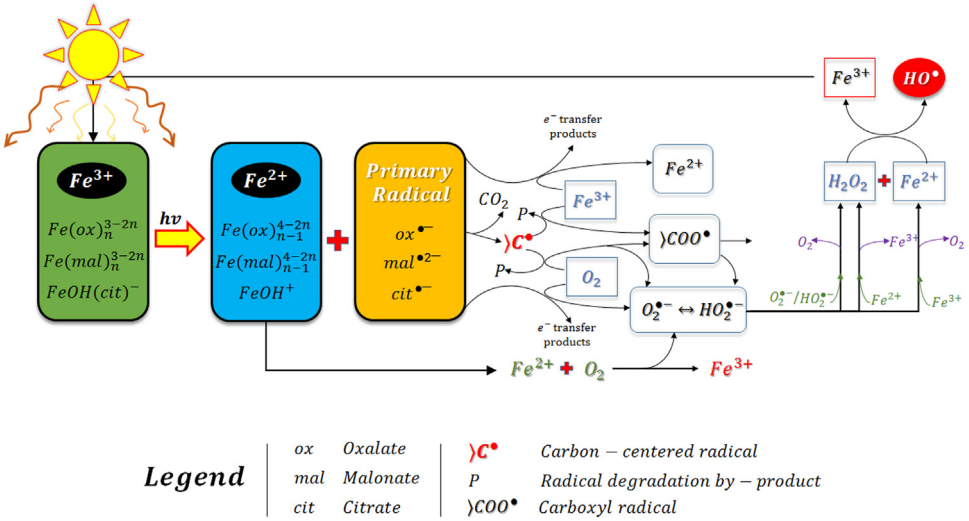

Fig. 8. Iron cycling in natural waters (adapted from [241]). The LMCT with oxalate, malonate and citrate complexes is presented, as indicative organic ligands of iron. Their photo-induced LMCT leads to reduced iron (blue panel) and ligand radicals (yellow panel). The ligand radicals initiate further oxidative-related reactions including the formation of H_2O_2, oxido-reduction of Fe, and $HO^{\bullet}$ generation. (For interpretation of the references to color in this figure legend, the reader is referred to the web version of this article.)

5.1.3.3. Event 3: triplet state energy transfer. The ^{3}DOM* can react in lesser extent with ground state DOM present in water, by energy/electron transfer and/or hydrogen transfer [330]. The end-product of this reaction is the formation of DOM radicals and oxidized organic matter.

8.1.3.4. Event 4: formation of $HO_2^{\bullet}/O_2^{\bullet-}$*, as* H_2O_2 *precursors.* Continuing with energy/electron transfers, reaction of the DOM radical with molecular oxygen will induce the production of reactive transient species, precursors of ROS, such as $HO_2^{\bullet}/O_2^{\bullet-}$ .The most important reaction of these transient species is their dismutation, where H_2O_2 is formed [331–334]. During daytime, the maximal concentrations of H_2O_2 were measured [335]. The type of DOM did not seem to influence the H_2O_2 production [332,336–340]. The initiator of the reaction is then oxidized.

5.1.3.4. Event 5: iron participation. Iron can complex with the organic matter forming stable Fe^{3+}-DOM species. Fe-DOM species are less prone to precipitation, and they have high absorption coefficients in near UV and visible range [257]; LMCT is therefore facilitated, between iron and DOM as a ligand. More specifically, below 450 nm, Fe-humic complexes absorb light strongly [240,270] and above 450 nm very few instances have been reported where efficient LMCT is taking place [262]. The reaction includes the reduction of iron and the oxidation of the participating ligand (DOM as ligand) as follows [341]:

$$Fe^{3+} - (DOM)_n + hv Fe^{2+} - (DOM)_{(n-1)} + DOM_{ox}^{+} \quad \text{(IV.3)}$$

Humic and fulvic acids can induce this reaction in the dark, but the reaction constant is greatly enhanced under illumination [234,240,342,343]. Even more, the presence of oxalate or malonate offer even higher reaction constants [241].

5.1.3.5. Event 6: the Fenton reaction. The Fenton reaction between the Fe^{2+} deriving from the LMCT and the H_2O_2 formed by the dismutation of hydroperoxyl and/or superoxide radicals leads to the production of $HO^{\bullet}$ and Fe^{3+} [18,239,341,344,345]. Fe^{3+} could re-complex with organic matter due to its strong electrophilic character.

5.1.3.6. Event 7: alternative Fe^{2+} *oxidation pathways.* Apart from the classical oxidation of Fe^{2+} to Fe^{3+} with H_2O_2 as oxidant, more pathways exist which produce Fe^{3+}. The reaction of Fe^{2+} with $HO_2^{\bullet}/O_2^{\bullet-}$ will produce Fe^{3+} but actually catalyzes the production of H_2O_2 [270,335,346]:

$$Fe^{2+} + O_2^{\bullet-} Fe^{3+} + H_2O_2 \quad \text{(IV.4)}$$

The advantage of this process is the active replenishment of the H_2O_2 in the bulk, which aids the $HO^{\bullet}$ production of Event 6.

5.1.3.7. Event 8: reduction of Fe^{3+} *to* Fe^{2+} *(Non-LMCT pathway).* Apart from the typical photo-Fenton-related pathways of iron reduction and re-initiation of the reactions, an alternative pathway has been reported. A reduced ligand L′ reacts with dissolved Fe^{3+} producing Fe^{2+} [239]:

$$Fe^{3+} + L' \rightarrow Fe^{2+} + L'_{ox} \quad \text{(IV.5)}$$

Other pathways include the reaction of Fe^{3+} with the amphoteric $HO_2^{\bullet}/O_2^{\bullet-}$, producing Fe^{2+} [238,239,241,262,270,347,348], in an inverse process compared with the one presented in event 7:

$$Fe^{3+} + O_2^{\bullet-} Fe^{2+} + O_2 \quad \text{(IV.6)}$$

The Fenton reaction could then be again initiated anew.

5.1.3.8. Event 9: release of Fe^{2+}/Fe^{3+} *from iron oxides and vice-versa.* Voelker et al. [270] have included in the potential mechanisms the release of iron into the bulk, through iron oxides. This plausible mechanism will result to "readily available" or "complexable" iron. Since the presence of oxygen is highly probable and the pH of the majority of natural waters is circumneutral, the influence of the iron oxides is to be considered (and will further be assessed in next steps). Also, if microorganisms are present, chelating substances (siderophores) can aid the (photo)dissolution of iron oxides [281].

5.1.3.9. Event 10: $Fe^{2+} - Fe^{3+}$ *cycling at the surface of the iron oxide.* Fe^{2+} at the surface of the iron oxide can react with the H_2O_2 formed in the bulk, producing $HO^{\bullet}$ and Fe^{3+} [270]. This reaction can be important, If dissolved Fe^{2+} has very low concentration [349].

5.1.3.10. Event 11: DOM-oxides complex. DOM can form complexes with the Fe oxides surface. More specifically, humic and carboxylate

substances can form complexes with the surface of the oxides and participate in LMCT [240,350]. Similarly to the Fe-DOM complexes in the bulk, the result is reduction of Fe^{3+} in the surface of the oxide, with simultaneous Fe^{2+} and oxidized ligand production.

5.1.3.11. Event 12: reaction of DOM with molecular oxygen. An additional, but less important reaction under concurrent illumination in presence of oxygen and DOM, is the reduction of dioxygen by CDOM, resulting to oxidized DOM and $HO_2^{\bullet}/O_2^{\bullet-}$, as follows [341]:

$$DOM + O_2 + h\nu \rightarrow DOM_{ox}^{+} + O_2^{\bullet-} \quad \text{(IV.7)}$$

The $HO_2^{\bullet}/O_2^{\bullet-}$ pair can then further regulate iron stoichiometry, as well as H_2O_2 production through dismutation.

Event 13: scavenging of $\boldsymbol{HO^{\bullet}}$ *by DOM.* Apart from the role of facilitator, DOM can equally play the role of scavenger in aquatic photochemistry, as follows [322,351,352]:

$$DOM + HO^{\bullet} \rightarrow DOM_{ox}^{+} + OH^{-} \quad \text{(IV.8)}$$

As it can be understood, since the hydroxyl radicals are highly reactive and non-selective, their harnessing for bacterial inactivation only, is impossible. Side reactions, such as with DOM, are bound to happen, but are a function of the type of DOM.

5.1.3.12. Event 14: restarting the DOM cycle. The oxidized DOM and ligands most possibly do not stop their contribution at the moment of oxidation. It has been reported that $HO^{\bullet}$ can cause fragmentation of the humic acids in water [344], and end up in lower molecular weight organic compounds [237,353–355]. These fragments can possibly re-complex with iron and further participate in the photo-chemical cycle. This process however is not infinite, and is macroscopically perceived as discoloration of CDOM, and this photobleaching has the side-effect of decreasing the absorption coefficients of water [356,357].

5.1.4. The dual role of DOM

In many works, the presence of DOM in water has been found to enhance the photo-Fenton reaction [27,346,358–366]. On the other hand, DOM has also been found to hinder the process [53,367,368]. Some authors suggested that the presence of humic substances inhibited [369–371] or had no significant effect [372–374] on the Fenton processes [362] (Fig. 9).

In overall, the ability of DOM to enhance or inhibit the photo-Fenton reaction depends primarily on the complexation capabilities, the efficiency of Fe^{2+}/Fe^{3+} cycling and the types of ROS produced during illumination [375]. As a principal, allochthonous fulvic acid is a less efficient producer of $^3DOM^*$ than autochthonous fulvic acid, while their ability to induce radicals is inversed [376]. Also, terrestrial DOM is inhibiting $HO^{\bullet}$ production more than the aquatic DOM [377], depending on their structure. Nevertheless, during solar disinfection of drinking water, the self-degradation of DOM is not a complete side-effect, since there is requirement to reduce the organics content; hence, the in-situ photo-Fenton reaction can achieve efficient disinfection and simultaneous DOM degradation/modification.

5.1.5. Other radical species and interactions

Apart from the DOM-related interactions, the ROS formed during the previous process can either attack the microorganisms, the DOM itself (self-scavenging) or even anions and inorganic substances present in water. For instance, the $HO^{\bullet}$ radicals formed can attack chloride ions, generating various chlorine radicals (in acidic solutions), such as $^{\bullet}Cl_2$, $^{\bullet}Cl_2^{-}$, or $ClOH$ [378]. Even more, hypochlorous acid can be formed from the reaction with H_2O_2. This would have the positive side-effect of inducing further inactivation. On the other hand, these reactions, or similar ones with bromine could potentially lead to halogenated by-products. Furthermore, the production of $HO^{\bullet}$ has been linked with nitrite and nitrate photo-reactions [379,380]. The reaction scheme is as follows [381]:

$$NO_3^{-} + H^{+} + h\nu \rightarrow HO^{\bullet} + {}^{\bullet}NO_2 \quad \text{(IV.9)}$$

$$NO_3^{-} + H_2O + h\nu \rightarrow HO^{\bullet} + NO_2^{-} + OH^{-} \quad \text{(IV.10)}$$

$$NO_2^{-} + H_2O + h\nu \rightarrow HO^{\bullet} + NO + OH^{-} \quad \text{(IV.11)}$$

$^{\bullet}NO_2$ is a nitrating agent in aqueous solutions, withholding potentially mutagenic nitroderivatives from phenolic compounds [382]. Also, photolysis of nitrogen-containing DOM is found to produce nitrite, as well as nitrate photolysis [366]. However, although nitrites are of less importance than nitrates in the overall photochemistry, their quantum yield is much higher [330]. The composition of the nitrogen-related compounds themselves is a dynamic process, changing during the photo-Fenton process, as it was reported [51], by the following reaction:

$$NH_4^{+} \leftrightarrow NH_3 + HO^{\bullet} \rightarrow NH_2OH \rightarrow NOH \rightarrow NO_2^{-} \leftrightarrow NO_3^{-} \quad \text{(IV.12)}$$

The reaction then continues as Eqs. (IV.9)–(IV.11) indicates.

Finally, the reaction of ROS with (bi)carbonates should not be overlooked, as they scavenge ROS, offering a protective effect on bacteria. HCO_3^{-} itself absorbs light, shielding the microorganisms along with the ROS-scavenging effect [204,383–385]. The reactions involved are as follows [47]:

$$HO^{\bullet} + HCO_3^{-} \rightarrow {}^{\bullet}CO_3^{-} + H_2O \quad \text{(IV.13)}$$

$$HO^{\bullet} + CO_3^{2-} \rightarrow {}^{\bullet}CO_3^{-} + OH^{-} \quad \text{(IV.14)}$$

However, the importance of the organic matter, ions and inorganic matter will be further assessed in a wastewater matrix, where the weight and contribution to either scavenging or producing ROS will be explained. In natural waters, either the positive or negative effects are not negligible, but great modifications are expected in wastewater.

6. Chapter VI: Provisional conclusions

In this review, we attempted to approach bacterial inactivation by the near-neutral photo-Fenton process in aqueous media, in an inside-out approach. We began by the description of the effect of light alone on different components of the bacterial cell (solar disinfection), followed by the individual responses of the Fenton reagents inside the bacteria, concluding with a contextualization in natural conditions.

As solar light has been proven to play a key role in the process, a significant part of the review is devoted to the elucidation of its inactivation mechanisms, which in fact share common ground and overlap significantly with the Fenton process. As a matter of fact, it is here proven that solar disinfection is indeed a multi-level photo-Fenton process, internally and possibly in the exterior of the microorganism.

The contents of this first part could be carefully extrapolated to other microorganisms as well. For instance, as the majority of the works has used *E. coli* as model microorganism, it is natural to use it as key reference for bacterial inactivation. Nevertheless, as other microorganisms share similar traits with the gram-Negative bacteria, the mechanisms could be extended to explain other species. A successful example on yeast model pathogen has been demonstrated, and the matrix effects in viral inactivation have been recently published and referenced herein.

In the following part of the review (Part 2), the applications on drinking water and wastewater are reviewed, presented in a critical

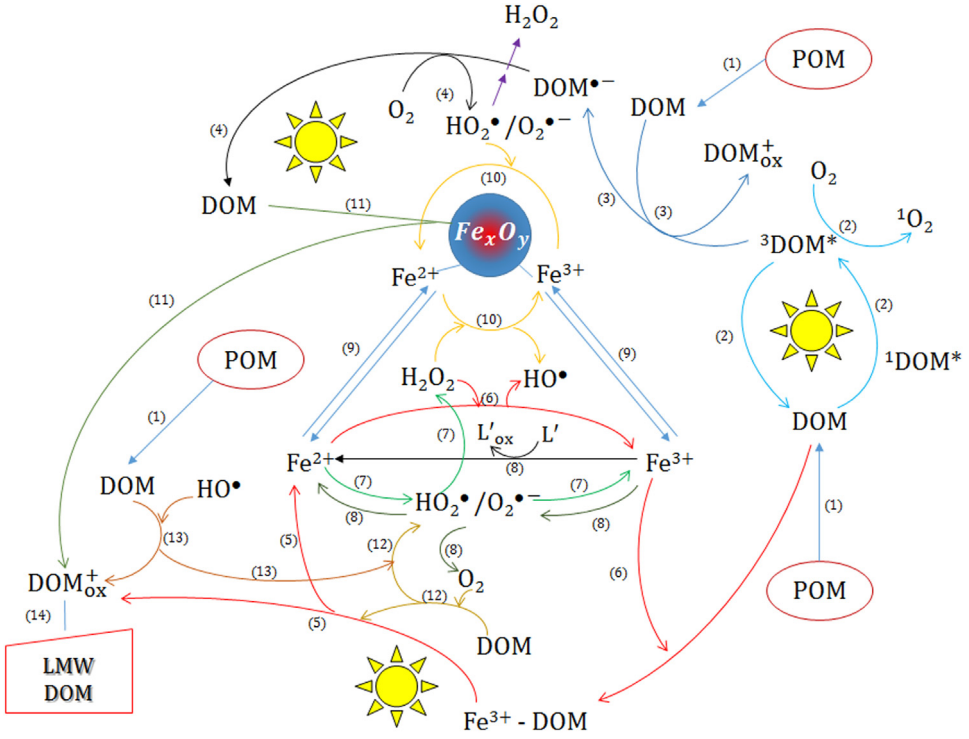

Fig. 9. Overall contribution of the natural water matrix and photochemical conversions. More detailed explanations can be found in-text, presented in events 1–14. DOM: Dissolved organic matter, ^{1}DOM*: singlet state DOM, ^{3}DOM*: triplet state DOM, **DOM$^+_{ox}$**: oxidized DOM, LMW DOM: low molecular weight DOM, **L′**: reduced ligand, **L′$_{ox}$**: oxidized reduced ligand, POM: particulate organic matter.

way, thus differentiating the principal components involved in each of the two contexts.

Acknowledgments

The authors wish to thank the Swiss Agency for Development and Cooperation (SDC) and the Swiss National Foundation for the Research for Development (r4d) Grant, for the funding through the project "Treatment of the hospital wastewaters in Côte d'Ivoire and in Colombia by advanced oxidation processes" (Project No. 146919), the Ministry for Economy and Competitiveness (Spanish Government) CTQ2013-46398-R and CTQ2014-54563-C3, the European Regional Development Fund (ERDF) and the European project WATERSPOUTT H2020-Water-5c-2015 (GA 688928) for the financial support. Finally, the authors wish to thank the reviewers for their deep and meaningful suggestions.

References

[1] K. Barbusiński, Chem. Dydakt. Ekol. Metrol. 1 (2009) 111–112.
[2] H. Fenton, J. Chem. Soc. Trans. 65 (1894) 899–910.
[3] S. Goldstein, D. Meyerstein, G. Czapski, Free Radical Biol. Med. 15 (1993) 435–445.
[4] M. Masarwa, H. Cohen, D. Meyerstein, D.L. Hickman, A. Bakac, J.H. Espenson, J. Am. Chem. Soc. 110 (1988) 4293–4297.
[5] P. Wardman, L.P. Candeias, Radiat. Res. 145 (1996) 523–531.
[6] W.C. Bray, M.H. Gorin, J. Am. Chem. Soc. 54 (1932) 2124–2125.
[7] F. Haber, J. Weiss, Proc. R. Soc. London A: Math. Phys. Eng. Sci. (1934) 332–351.
[8] M. Kremer, Phys. Chem. Chem. Phys. 1 (1999) 3595–3605.
[9] W. Barb, J. Baxendale, P. George, K. Hargrave, Nature 163 (1949) 692–694.
[10] J. Baxendale, M. Evans, C. Park, Trans. Faraday Soc. 42 (1946) 155–169.
[11] C. Walling, Acc. Chem. Res. 8 (1975) 125–131.
[12] C. Walling, G.M. Ei-Taliawi, J. Am. Chem. Soc. 95 (1973) 844–847.
[13] C. Walling, G. El-Taliawi, J. Am. Chem. Soc. 95 (1973) 848–850.
[14] C. Walling, R.A. Johnson, J. Am. Chem. Soc. 97 (1975) 2405–2407.
[15] C. Walling, R.A. Johnson, J. Am. Chem. Soc. 97 (1975) 363–367.
[16] C. Walling, S. Kato, J. Am. Chem. Soc. 93 (1971) 4275–4281.
[17] J.A. Imlay, S. Linn, Science 240 (1988) 1302–1309.
[18] R.G. Zepp, B.C. Faust, J. Holgné, Environ. Sci. Technol. 26 (1992) 313–319.
[19] R. Bauer, Chemosphere 29 (1994) 1225–1233.
[20] J. Kiwi, C. Pulgarin, P. Peringer, M. Grätzel, Appl. Catal. B: Environ. 3 (1993) 85–99.
[21] G. Ruppert, R. Bauer, G. Heisler, Chemosphere 28 (1994) 1447–1454.
[22] M. Cho, Y. Lee, H. Chung, J. Yoon, Appl. Environ. Microbiol. 70 (2004) 1129–1134.
[23] A.-G. Rincón, C. Pulgarin, Appl. Catal. B: Environ. 63 (2006) 222–231.
[24] A.-G. Rincón, C. Pulgarin, Catal. Today 124 (2007) 204–214.
[25] A.-G. Rincón, C. Pulgarin, Catal. Today 122 (2007) 128–136.
[26] A. Moncayo-Lasso, R.A. Torres-Palma, J. Kiwi, N. Benítez, C. Pulgarin, Appl. Catal. B: Environ. 84 (2008) 577–583.
[27] A. Moncayo-Lasso, J. Sanabria, C. Pulgarin, N. Benitez, Chemosphere 77 (2009) 296–300.
[28] I. Kim, H. Tanaka, Environ. Int. 35 (2009) 793–802.
[29] F. Mazille, A. Moncayo-Lasso, D. Spuhler, A. Serra, J. Peral, N. Benítez, C. Pulgarin, Chem. Eng. J. 160 (2010) 176–184.
[30] F. Sciacca, J.A. Rengifo-Herrera, J. Wéthé, C. Pulgarin, Chemosphere 78 (2010) 1186–1191.
[31] D. Spuhler, J. Andrés Rengifo-Herrera, C. Pulgarin, Appl. Catal. B: Environ. 96 (2010) 126–141.
[32] J.I. Nieto-Juarez, K. Pierzchła, A. Sienkiewicz, T. Kohn, Environ. Sci. Technol. 44 (2010) 3351–3356.
[33] F. Sciacca, J.A. Rengifo-Herrera, J. Wéthé, C. Pulgarin, Sol. Energy 85 (2011) 1399–1408.
[34] E.R. Bandala, L. González, F. De la Hoz, M.A. Pelaez, D.D. Dionysiou, P.S. Dunlop, J.A. Byrne, J.L. Sanchez, J. Photochem. Photobiol. A: Chem. 218 (2011) 185–191.
[35] A. Bernabeu, R. Vicente, M. Peribáñez, A. Arques, A. Amat, Chem. Eng. J. 171 (2011) 490–494.
[36] E. Ortega-Gomez, P. Fernandez-Ibanez, M.M. Ballesteros Martin, M.I. Polo-Lopez, B. Esteban Garcia, J.A. Sanchez Perez, Water Res. 46 (2012) 6154–6162.
[37] A. Moncayo-Lasso, L.E. Mora-Arismendi, J.A. Rengifo-Herrera, J. Sanabria, N. Benítez, C. Pulgarin, Photochem. Photobiol. Sci. 11 (2012) 821–827.
[38] M.I. Polo-López, I. García-Fernández, T. Velegraki, A. Katsoni, I. Oller, D. Mantzavinos, P. Fernández-Ibáñez, Appl. Catal. B: Environ. 111 (2012) 545–554.
[39] N. Klamerth, S. Malato, A. Agüera, A. Fernández-Alba, G. Mailhot, Environ. Sci. Technol. 46 (2012) 2885–2892.
[40] I. García-Fernández, M. Polo-López, I. Oller, P. Fernández-Ibáñez, Appl. Catal. B: Environ. 121 (2012) 20–29.
[41] E.R. Bandala, L. González, J.L. Sanchez-Salas, J.H. Castillo, J. Water Health 10 (2012) 20–30.

[42] J. Rodríguez-Chueca, M. Morales, R. Mosteo, M. Ormad, J. Ovelleiro, Photochem. Photobiol. Sci. 12 (2013) 864–871.
[43] E. Ortega-Gómez, B. Esteban García, M.M. Ballesteros Martín, P. Fernández Ibáñez, J.A. Sánchez Pérez, Catal. Today 209 (2013) 195–200.
[44] J.I. Nieto-Juarez, T. Kohn, Photochem. Photobiol. Sci. 12 (2013) 1596–1605.
[45] J. Ndounla, D. Spuhler, S. Kenfack, J. Wéthé, C. Pulgarin, Appl. Catal. B: Environ. 129 (2013) 309–317.
[46] M. Agulló-Barceló, M. Polo-López, F. Lucena, J. Jofre, P. Fernández-Ibáñez, Appl. Catal. B: Environ. 136 (2013) 341–350.
[47] D. Rubio, E. Nebot, J.F. Casanueva, C. Pulgarin, Water Res. 47 (2013) 6367–6379.
[48] M.I. Polo-López, I. Oller, P. Fernández-Ibáñez, Catal. Today 209 (2013) 181–187.
[49] C. Ruales-Lonfat, A.V. López, J.F. Barona, A. Moncayo-Lasso, N.B. Vásquez, C. Pulgarín, Technologies for Sustainable Development, Springer, 2014, pp. 113–128.
[50] C. Ruales-Lonfat, N. Benítez, A. Sienkiewicz, C. Pulgarín, Appl. Catal. B: Environ. 160 (2014) 286–297.
[51] J. Ndounla, C. Pulgarin, Sci. Total Environ. 493 (2014) 229–238.
[52] J. Ndounla, S. Kenfack, J. Wéthé, C. Pulgarin, Appl. Catal. B: Environ. 148–149 (2014) 144–153.
[53] E. Ortega-Gómez, M.M. Ballesteros Martín, B. Esteban García, J.A. Sánchez Pérez, P. Fernández Ibáñez, Appl. Catal. B: Environ. 148–149 (2014) 484–489.
[54] E. Ortega-Gómez, B.E. García, M.B. Martín, P.F. Ibáñez, J.S. Pérez, Water Res. 63 (2014) 316–324.
[55] A. Teodoro, M.Á. Boncz, A.M. Júnior, P.L. Paulo, J. Environ. Chem. Eng. 2 (2014) 958–962.
[56] J. Rodríguez-Chueca, A. Mediano, M. Ormad, R. Mosteo, J. Ovelleiro, Water Res. 60 (2014) 250–258.
[57] J. Rodríguez-Chueca, M. Polo-López, R. Mosteo, M. Ormad, P. Fernández-Ibáñez, Appl. Catal. B: Environ. 150 (2014) 619–629.
[58] M.I. Polo-López, M. Castro-Alférez, I. Oller, P. Fernández-Ibáñez, Chem. Eng. J. 257 (2014) 122–130.
[59] C. Ruales-Lonfat, J.F. Barona, A. Sienkiewicz, M. Bensimon, J. Vélez-Colmenares, N. Benítez, C. Pulgarín, Appl. Catal. B: Environ. 166–167 (2015) 497–508.
[60] S. Giannakis, S. Papoutsakis, E. Darakas, A. Escalas-Cañellas, C. Pétrier, C. Pulgarin, Ultrason. Sonochem. 22 (2015) 515–526.
[61] E. Ortega-Gómez, M.M. Ballesteros Martín, A. Carratalà, P. Fernández Ibañez, J.A. Sánchez Pérez, C. Pulgarín, Appl. Catal. B: Environ. 174–175 (2015) 395–402.
[62] S. Barreca, J.J. Velez Colmenares, A. Pace, S. Orecchio, C. Pulgarin, J. Environ. Chem. Eng. 3 (2015) 317–324.
[63] C. Pulgarin, CHIMIA Int. J. Chem. 69 (2015) 7–9.
[64] J. Ndounla, C. Pulgarin, Solar light (hv) and H_2O_2/hv photo-disinfection of natural alkaline water (pH 8. 6) in a compound parabolic collector at different day periods in Sahelian region, Environ. Sci. Pollut. Res. 22 (21) (2015) 17082–17094.
[65] J. Rodríguez-Chueca, M.P. Ormad, R. Mosteo, J.L. Ovelleiro, Chem. Eng. Sci. 138 (2015) 730–740.
[66] J. Rodríguez-Chueca, M.P. Ormad, R. Mosteo, J. Sarasa, J.L. Ovelleiro, Water Environ. Res. 87 (2015) 281–288.
[67] V. Aurioles-López, M.I. Polo-López, P. Fernández-Ibáñez, A. López-Malo, E.R. Bandala, Effect of iron salt counter ion in dose-response curves for inactivation of Fusarium solani in water through solar driven Fenton-like processes, Phys. Chem. Earth Parts A/B/C 91 (2016) 46–52.
[68] C. Ruales-Lonfat, J.F. Barona, A. Sienkiewicz, J. Vélez, L.N. Benítez, C. Pulgarín, Appl. Catal. B: Environ. 180 (2016) 379–390.
[69] A. Ruiz-Aguirre, M.I. Polo-López, P. Fernández-Ibáñez, G. Zaragoza, Desalin. Water Treat. 55 (2015) 2792–2799.
[70] E. Ortega-Gómez, M.B. Martín, B.E. García, J.S. Pérez, P.F. Ibáñez, Appl. Catal. B: Environ. 181 (2016) 1–6.
[71] S. Giannakis, C. Ruales-Lonfat, S. Rtimi, S. Thabet, P. Cotton, C. Pulgarin, Appl. Catal. B: Environ. 185 (2016) 150–162.
[72] R.B. Setlow, Proc. Natl. Acad. Sci. U. S. A. 71 (1974) 3363–3366.
[73] E.G. Mbonimpa, B. Vadheim, E.R. Blatchley 3rd, Water Res. 46 (2012) 2344–2354.
[74] R. Bensasson, E. Land, T. Truscott, Excited States and Free Radicals in Biology and Medicine: Contributions from Flash Photolysis and Pulse Radiolysis, Oxford University Press, 1993.
[75] D.I. Pattison, M.J. Davies, Cancer: Cell Structures, Carcinogens and Genomic Instability, Springer, 2006, pp. 131–157.
[76] H. Black, P. Forbes, J. Cleaver, H. Ananthaswamy, S. Ullrich, R. Tyrrell, J. Photochem. Photobiol. B: Biol. 40 (1997) 29–47.
[77] J. Cadet, C. Anselmino, T. Douki, L. Voituriez, J. Photochem. Photobiol. B: Biol. 15 (1992) 277–298.
[78] J.-L. Ravanat, T. Douki, J. Cadet, J. Photochem. Photobiol. B: Biol. 63 (2001) 88–102.
[79] R.P. Sinha, D.-P. Häder, Photochem. Photobiol. Sci. 1 (2002) 225–236.
[80] T. Douki, G. Laporte, J. Cadet, Nucleic Acids Res. 31 (2003) 3134–3142.
[81] D.L. Mitchell, R.S. Nairn, Photochem. Photobiol. 49 (1989) 805–819.
[82] G.P. Pfeifer, Photochem. Photobiol. 65 (1997) 270–283.
[83] G.P. Pfeifer, Y.-H. You, A. Besaratinia, Mutat. Res. 571 (2005) 19–31.
[84] J.-H. Yoon, C.-S. Lee, T.R. O'Connor, A. Yasui, G.P. Pfeifer, J. Mol. Biol. 299 (2000) 681–693.
[85] J.S. Taylor, M.P. Cohrs, J. Am. Chem. Soc. 109 (1987) 2834–2835.
[86] J.S. Taylor, H.F. Lu, J.J. Kotyk, Photochem. Photobiol. 51 (1990) 161–167.
[87] K. Wierzchowski, D. Shugar, Acta Biochim. Pol. 8 (1960) 219–234.
[88] T. Douki, J. Cadet, Biochemistry 40 (2001) 2495–2501.
[89] J.M. Song, J. Milligan, B.M. Sutherland, Biochemistry 41 (2002) 8683–8688.
[90] M.J. Davies, Biochem. Biophys. Res. Commun. 305 (2003) 761–770.
[91] A. Eisenstark, Mutat. Res. 422 (1998) 85–95.
[92] H.-L. Lo, S. Nakajima, L. Ma, B. Walter, A. Yasui, D.W. Ethell, L.B. Owen, BMC Cancer 5 (2005) 135.
[93] W.P. Roos, B. Kaina, Trends Mol. Med. 12 (2006) 440–450.
[94] O. Sidorkina, S. Kuznetsov, J. Blais, M. Bazin, J. Laval, R. Santus, Photochem. Photobiol. 69 (1999) 658–663.
[95] M.J. Davies, R.J. Truscott, J. Photochem. Photobiol. B: Biol. 63 (2001) 114–125.
[96] Y. Matsumura, H.N. Ananthaswamy, Toxicol. Appl. Pharmacol. 195 (2004) 298–308.
[97] T. Douki, A. Reynaud-Angelin, J. Cadet, E. Sage, Biochemistry 42 (2003) 9221–9226.
[98] P.J. Rochette, J.P. Therrien, R. Drouin, D. Perdiz, N. Bastien, E.A. Drobetsky, E. Sage, Nucleic Acids Res. 31 (2003) 2786–2794.
[99] A. Besaratinia, T.W. Synold, H.-H. Chen, C. Chang, B. Xi, A.D. Riggs, G.P. Pfeifer, Proc. Natl. Acad. Sci. U. S. A. 102 (2005) 10058–10063.
[100] L.F. Batista, B. Kaina, R. Meneghini, C.F. Menck, Mutat. Res. 681 (2009) 197–208.
[101] Y. Jiang, M. Rabbi, M. Kim, C. Ke, W. Lee, R.L. Clark, P.A. Mieczkowski, P.E. Marszalek, Biophys. J. 96 (2009) 1151–1158.
[102] S. Mouret, C. Philippe, J. Gracia-Chantegrel, A. Banyasz, S. Karpati, D. Markovitsi, T. Douki, Org. Biomol. Chem. 8 (2010) 1706–1711.
[103] A. Emrick, J. Sutherland, Photochem. Photobiol. 49 (1989) 35S.
[104] S.E. Freeman, H. Hacham, R. Gange, D. Maytum, J.C. Sutherland, B. Sutherland, Proc. Natl. Acad. Sci. U. S. A. 86 (1989) 5605–5609.
[105] H. Hacham, S.E. Freeman, R.W. Gange, D.J. Maytum, J.C. Sutherland, B.M. Sutherland, Photochem. Photobiol. 52 (1990) 893–896.
[106] F. Quaite, B.M. Sutherland, J.C. Sutherland, Nature 358 (1992) 576–578.
[107] J. Cadet, E. Sage, T. Douki, Mutat. Res. 571 (2005) 3–17.
[108] J. Cadet, M. Berger, T. Douki, B. Morin, S. Raoul, J. Ravanat, S. Spinelli, Biol. Chem. 378 (1997) 1275–1286.
[109] C.S. Foote, Photochem. Photobiol. 54 (1991) 659.
[110] J. Cadet, R. Teoule, Photochem. Photobiol. 28 (1978) 661–665.
[111] C. Sheu, C.S. Foote, J. Am. Chem. Soc. 115 (1993) 10446–10447.
[112] J. Hoerter, A. Pierce, C. Troupe, J. Epperson, A. Eisenstark, Photochem. Photobiol. 64 (1996) 537–541.
[113] E. Smyk-Randall, O. Brown, A. Wilke, A. Eisenstark, D. Flint, Free Radical Biol. Med. 14 (1993) 609–613.
[114] C. Kielbassa, L. Roza, B. Epe, Carcinogenesis 18 (1997) 811–816.
[115] D.E. Heck, M. Shakarjian, H.D. Kim, J.D. Laskin, A.M. Vetrano, Ann. N. Y. Acad. Sci. 1203 (2010) 120–125.
[116] D.E. Heck, A.M. Vetrano, T.M. Mariano, J.D. Laskin, J. Biol. Chem. 278 (2003) 22432–22436.
[117] A. Eisenstark, G. Perrot, Mol. Gen. Genet. MGG 207 (1987) 68–72.
[118] S. Kawanishi, T. Hiraku, Oxidants and Antioxidants in Cutaneous Biology. Curr Probl Dermatol., vol. 29, Karger, Basel, 2001, pp. 74–82.
[119] J.L. Ravanat, C. Saint-Pierre, P. Di Mascio, G.R. Martinez, M.H. Medeiros, J. Cadet, Helv. Chim. Acta 84 (2001) 3702–3709.
[120] A.L. Santos, V. Oliveira, I. Baptista, I. Henriques, N.C. Gomes, A. Almeida, A. Correia, Â. Cunha, Arch. Microbiol. 195 (2013) 63–74.
[121] F. Bosshard, M. Bucheli, Y. Meur, T. Egli, Microbiology 156 (2010) 2006–2015.
[122] J.A. Imlay, Annu. Rev. Microbiol. 57 (2003) 395–418.
[123] A. Ligeza, A.N. Tikhonov, J.S. Hyde, W.K. Subczynski, Biochim. Biophys. Acta 1365 (1998) 453–463.
[124] V. Massey, S. Strickland, S.G. Mayhew, L.G. Howell, P. Engel, R.G. Matthews, M. Schuman, P. Sullivan, Biochem. Biophys. Res. Commun. 36 (1969) 891–897.
[125] J.A. Imlay, Annu. Rev. Biochem. 77 (2008) 755.
[126] B. González-Flecha, B. Demple, J. Biol. Chem. 270 (1995) 13681–13687.
[127] J. Imlay, I. Fridovich, J. Biol. Chem. 266 (1991) 6957–6965.
[128] J.A. Imlay, J. Biol. Chem. 270 (1995) 19767–19777.
[129] K.R. Messner, J.A. Imlay, J. Biol. Chem. 274 (1999) 10119–10128.
[130] V. Massey, J. Biol. Chem. 269 (1994) 22459–22462.
[131] L.C. Seaver, J.A. Imlay, J. Bacteriol. 183 (2001) 7173–7181.
[132] J.D. Hoerter, A.A. Arnold, D.A. Kuczynska, A. Shibuya, C.S. Ward, M.G. Sauer, A. Gizachew, T.M. Hotchkiss, T.J. Fleming, S. Johnson, J. Photochem. Photobiol. B: Biol. 81 (2005) 171–180.
[133] P. Chelikani, I. Fita, P.C. Loewen, Cell. Mol. Life Sci. 61 (2004) 192–208.
[134] J. Cadet, DNA damage caused by oxidation, deamination, of ultraviolet radiation and photoexcited psoralens in DNA adducts, in: K. Hemminki, A. Dipple, Dep Shuker, F.f. Kadlubar, D. Segerbäck, H. Bartsch (Eds.), Identification and Biological Significance, International Agency for Research on Cancer, IARC Scientific Publication No 125, Lyon, 1994, pp. 245–276.
[135] J. Cadet, T. Delatour, T. Douki, D. Gasparutto, J.-P. Pouget, J.-L. Ravanat, S. Sauvaigo, Mutat. Res. 424 (1999) 9–21.
[136] J.M. McCord, I. Fridovich, J. Biol. Chem. 244 (1969) 6049–6055.
[137] S.S. Korshunov, J.A. Imlay, Mol. Microbiol. 43 (2002) 95–106.
[138] R.E. Lynch, I. Fridovich, J. Biol. Chem. 253 (1978) 4697–4699.
[139] S. Burney, J.L. Caulfield, J.C. Niles, J.S. Wishnok, S.R. Tannenbaum, Mutat. Res. 424 (1999) 37–49.
[140] W. Koppenol, J. Moreno, W.A. Pryor, H. Ischiropoulos, J. Beckman, Chem. Res. Toxicol. 5 (1992) 834–842.

[141] S.x. Chen, P. Schopfer, Eur. J. Biochem. 260 (1999) 726–735.
[142] A. Gomes, L. Asad, I. Felzenszwalb, A. Leitão, A. Silva, H. Guillobel, N. Asad, Radiat. Environ. Biophys. 43 (2004) 219–222.
[143] R.L. Knowles, A. Eisenstark, Environ. Health Perspect. 102 (1994) 88.
[144] S. Basu-Modak, R.M. Tyrrell, Cancer Res. 53 (1993) 4505–4510.
[145] R.M. Tyrrell, M. Pidoux, Photochem. Photobiol. 49 (1989) 407–412.
[146] R.M. Tyrrell, C.A. Pourzand, J. Brown, V. Hejmadi, V. Kvam, S. Ryter, R. Watkin, Radiat. Prot. Dosim. 91 (2000) 37–39.
[147] R.L. Levine, Free Radical Biol. Med. 32 (2002) 790–796.
[148] D. Touati, Arch. Biochem. Biophys. 373 (2000) 1–6.
[149] A. Bagg, J. Neilands, Microbiol. Rev. 51 (1987) 509.
[150] J.H. Crosa, Microbiol. Rev. 53 (1989) 517–530.
[151] K. Hantke, FEMS Microbiol. Lett. 44 (1987) 53–57.
[152] B. Morgan, O. Lahav, Chemosphere 68 (2007) 2080–2084.
[153] V. Braun, Int. J. Med. Microbiol. 291 (2001) 67–79.
[154] A.J. Hudson, S.C. Andrews, C. Hawkins, J.M. Williams, M. Izuhara, F.C. Meldrum, S. Mann, P.M. Harrison, J.R. Guest, Eur. J. Biochem. 218 (1993) 985–995.
[155] K. Keyer, J.A. Imlay, Proc. Natl. Acad. Sci. U. S. A. 93 (1996) 13635–13640.
[156] J. Yariv, A. Kalb, R. Sperling, E. Bauminger, S. Cohen, S. Ofer, Biochem. J. 197 (1981) 171–175.
[157] B. Halliwell, J. Gutteridge, Biochem. J. 219 (1984) 1.
[158] S.D. Aust, L.A. Morehouse, C.E. Thomas, J. Free Radicals Biol. Med. 1 (1985) 3–25.
[159] P. Biemond, A. Swaak, C.M. Beindorff, J.F. Koster, Biochem. J. 239 (1986) 169–173.
[160] P. Biemond, A.J. Swaak, H.G. van Eijk, J.F. Koster, Free Radical Biol. Med. 4 (1988) 185–198.
[161] J.A. Imlay, Mol. Microbiol. 59 (2006) 1073–1082.
[162] S. Jang, J.A. Imlay, J. Biol. Chem. 282 (2007) 929–937.
[163] S. Varghese, Y. Tang, J.A. Imlay, J. Bacteriol. 185 (2003) 221–230.
[164] L. Kelland, S. Moss, D. Davies, Photochem. Photobiol. 37 (1983) 617–622.
[165] J. Cadet, S. Mouret, J.L. Ravanat, T. Douki, Photochem. Photobiol. 88 (2012) 1048–1065.
[166] C. Pourzand, R.D. Watkin, J.E. Brown, R.M. Tyrrell, Proc. Natl. Acad. Sci. U. S. A. 96 (1999) 6751–6756.
[167] J. Cadet, M. Berger, T. Douki, J.-L. Ravanat, Reviews of Physiology Biochemistry and Pharmacology, vol. 131, Springer, 1997, pp. 1–87.
[168] D.R. Lloyd, D.H. Phillips, P.L. Carmichael, Chem. Res. Toxicol. 10 (1997) 393–400.
[169] K. Randerath, E. Randerath, C.V. Smith, J. Chang, Chem. Res. Toxicol. 9 (1996) 247–254.
[170] J.L. Farber, Environ. Health Perspect. 102 (1994) 17.
[171] G.W. Teebor, R.J. Boorstein, J. Cadet, Int. J. Radiat. Biol. 54 (1988) 131–150.
[172] W.K. Pogozelski, T.D. Tullius, Chem. Rev. 98 (1998) 1089–1108.
[173] J. Cadet, J.L. Ravanat, G.R. Martinez, M.H. Medeiros, P.D. Mascio, Photochem. Photobiol. 82 (2006) 1219–1225.
[174] F. Hutchinson, Prog. Nucleic Acid Res. Mol. Biol. 32 (1985) 115–154.
[175] J.A. Imlay, Curr. Opin. Microbiol. 24 (2015) 124–131.
[176] E. Bourdon, D. Blache, Antioxid. Redox Signaling 3 (2001) 293–311.
[177] H.-R. Shen, J.D. Spikes, C.J. Smith, J. Kopeček, J. Photochem. Photobiol. A: Chem. 133 (2000) 115–122.
[178] F. Bosshard, K. Riedel, T. Schneider, C. Geiser, M. Bucheli, T. Egli, Environ. Microbiol. 12 (2010) 2931–2945.
[179] E. Cabiscol, J. Tamarit, J. Ros, Int. Microbiol. 3 (2010) 3–8.
[180] F. Chiti, Protein, Misfolding, Aggregation, and Conformational Diseases, Springer, 2006, pp. 43–59.
[181] L. Fucci, C.N. Oliver, M.J. Coon, E.R. Stadtman, Proc. Natl. Acad. Sci. U. S. A. 80 (1983) 1521–1525.
[182] T. Grune, T. Jung, K. Merker, K.J. Davies, Int. J. Biochem. Cell Biol. 36 (2004) 2519–2530.
[183] T.C. Squier, Exp. Gerontol. 36 (2001) 1539–1550.
[184] E.R. Stadtman, Free Radical Biol. Med. 9 (1990) 315–325.
[185] Y.-J. Rang, J.D. Spikes, Arch. Biochem. Biophys. 172 (1976) 565–573.
[186] E. Silva, C. De Landea, A.M.a. Edwards, E. Lissi, J. Photochem. Photobiol. B: Biol. 55 (2000) 196–200.
[187] R. Pizarro, Int. J. Radiat. Biol. 68 (1995) 293–299.
[188] P.E. Morgan, R.T. Dean, M.J. Davies, Free Radical Biol. Med. 36 (2004) 484–496.
[189] C. Luxford, R.T. Dean, M.J. Davies, Chem. Res. Toxicol. 13 (2000) 665–672.
[190] K.B. Choksi, J. Papaconstantinou, Free Radical Biol. Med. 44 (2008) 1795–1805.
[191] R. Venkatadri, R.W. Peters, Hazard. Waste Hazard. Mater. 10 (1993) 107–149.
[192] J.A. Imlay, Annu. Rev. Biochem. 77 (2008) 755–776.
[193] L.C. Seaver, J.A. Imlay, J. Bacteriol. 183 (2001) 7182–7189.
[194] E. Cadenas, K.J. Davies, Free Radical Biol. Med. 29 (2000) 222–230.
[195] C. Sichel, P. Fernández-Ibáñez, M. de Cara, J. Tello, Water Res. 43 (2009) 1841–1850.
[196] J.A. Imlay, S. Linn, J. Bacteriol. 166 (1986) 519–527.
[197] L. Uhl, A. Gerstel, M. Chabalier, S. Dukan, Heliyon 1 (2015) e00049.
[198] B. Halliwell, O.I. Aruoma, FEBS Lett. 281 (1991) 9–19.
[199] S. Park, X. You, J.A. Imlay, Proc. Natl. Acad. Sci. U. S. A. 102 (2005) 9317–9322.
[200] S.I. Liochev, I. Fridovich, Free Radical Biol. Med. 16 (1994) 29–33.
[201] D. Touati, M. Jacques, B. Tardat, L. Bouchard, S. Despied, J. Bacteriol. 177 (1995) 2305–2314.
[202] B. Halliwell, J. Gutteridge, FEBS Lett. 307 (1992) 108–112.
[203] J. Rush, Z. Maskos, W. Koppenol, FEBS Lett. 261 (1990) 121–123.
[204] A.-G. Rincon, C. Pulgarin, Appl. Catal. B: Environ. 51 (2004) 283–302.
[205] H. Ananthaswamy, A. Eisenstark, Photochem. Photobiol. 24 (1976) 439–442.
[206] P. Hartman, A. Eisenstark, Mutat. Res. 72 (1980) 31–42.
[207] M. Fisher, C. Keenan, K. Nelson, B. Voelker, J. Water Health 6 (2008) 35–51.
[208] M.B. Fisher, M. Iriarte, K.L. Nelson, Water Res. 46 (2012) 1745–1754.
[209] P. Hartman, A. Eisenstark, J. Bacteriol. 133 (1978) 769–774.
[210] C. Keenan, The Effect of Additional Hydrogen Peroxide on Solar Water Disinfection, in Civil and Environmental Engineering, Massachusetts Institute of Technology, Cambridge, 2003, pp. 44.
[211] R. Khaengraeng, R. Reed, J. Appl. Microbiol. 99 (2005) 39–50.
[212] T.W. Ng, T. An, G. Li, W.K. Ho, H.Y. Yip, H. Zhao, P.K. Wong, J. Photochem. Photobiol. B: Biol. 149 (2015) 164–171.
[213] M.B. Fisher, K.L. Nelson, Appl. Environ. Microbiol. 80 (2014) 935–942.
[214] A.D. Bokare, W. Choi, J. Hazard. Mater. 275 (2014) 121–135.
[215] J. Pierre, M. Fontecave, R. Crichton, Biometals 15 (2002) 341–346.
[216] Wang Chuan, Hong Liu, Zhimin Sun. Heterogeneous photo-Fenton reaction catalyzed by nanosized iron oxides for water treatment, Int. J. Photoenergy (2012), 2012, 1-10.
[217] S.R. Pouran, A.A.A. Raman, W.M.A.W. Daud, J. Clean. Prod. 64 (2014) 24–35.
[218] J. De Laat, H. Gallard, Environ. Sci. Technol. 33 (1999) 2726–2732.
[219] W. Sung, J.J. Morgan, Environ. Sci. Technol. 14 (1980) 561–568.
[220] L. Demarchis, M. Minella, R. Nisticò, V. Maurino, C. Minero, D. Vione, J. Photochem. Photobiol. A: Chem. 307 (2015) 99–107.
[221] H. Bataineh, O. Pestovsky, A. Bakac, Chem. Sci. 3 (2012) 1594–1599.
[222] J. Gomis, R. Vercher, A. Amat, D. Mártire, M. González, A.B. Prevot, E. Montoneri, A. Arques, L. Carlos, Catal. Today 209 (2013) 176–180.
[223] C. Minero, M. Lucchiari, V. Maurino, D. Vione, RSC Adv. 3 (2013) 26443–26450.
[224] S.H. Lin, C.C. Lo, Water Res. 31 (1997) 2050–2056.
[225] E. Neyens, J. Baeyens, J. Hazard. Mater. 98 (2003) 33–50.
[226] R.M. Cornell, U. Schwertmann, The Iron Oxides: Structure, Properties, Reactions, Occurrences and Uses, John Wiley & Sons, 2006.
[227] J.P. Jolivet, C. Chanéac, E. Tronc, Chem. Commun. 10 (2004) 481–487.
[228] S.M. Kraemer, Aquat. Sci. 66 (2004) 3–18.
[229] W.Y. Guohua, Z. Hongying, W. Xiuchun, Y. Yujing, Prog. Chem. 8 (2013) 003.
[230] W. Feng, D. Nansheng, Chemosphere 41 (2000) 1137–1147.
[231] J.K. Leland, A.J. Bard, J. Phys. Chem. 91 (1987) 5076–5083.
[232] F. Millero, Water Sci. Technol. Lib. 25 (1997) 381–398.
[233] W. Stumm, B. Sulzberger, Geochim. Cosmochim. Acta 56 (1992) 3233–3257.
[234] Y. Deng, W. Stumm, Appl. Geochem. 9 (1994) 23–36.
[235] G.J. Jones, B.P. Palenik, F.M. Morel, J. Phycol. 23 (1987) 237–244.
[236] D.W. King, Environ. Sci. Technol. 32 (1998) 2997–3003.
[237] W.L. Miller, R.G. Zepp, Geophys. Res. Lett. 22 (1995) 417–420.
[238] B.M. Voelker, D.L. Sedlak, Mar. Chem. 50 (1995) 93–102.
[239] B.M. Voelker, B. Sulzberger, Environ. Sci. Technol. 30 (1996) 1106–1114.
[240] T.D. Waite, F.M. Morel, Environ. Sci. Technol. 18 (1984) 860–868.
[241] B.C. Faust, R.G. Zepp, Environ. Sci. Technol. 27 (1993) 2517–2522.
[242] T. Fox, N. Comerford, Soil Sci. Soc. Am. J. 54 (1990) 1139–1144.
[243] D. Grosjean, K. Van Cauwenberghe, J.P. Schmid, P.E. Kelley, J.N. Pitts Jr., Environ. Sci. Technol. 12 (1978) 313–317.
[244] K. Kawamura, S. Steinberg, I. Kaplan, Int. J. Environ. Anal. Chem. 19 (1985) 175–188.
[245] W.L. Lamar, D.F. Goerlitz, Organic Acids in Naturally Colored Surface Waters, USGPO, 1966.
[246] G.E. Likens, E.S. Edgerton, J.N. Galloway, Tellus B 35 (1983) 16–24.
[247] H. Satsumabayashi, H. Kurita, Y. Yokouchi, H. Ueda, Atmos. Environ. A Gen. Top. 24 (1990) 1443–1450.
[248] E.M. Thurman, Organic Geochemistry of Natural Waters, Springer Science & Business Media, 2012.
[249] Y. Zuo, J. Hoigne, Environ. Sci. Technol. 26 (1992) 1014–1022.
[250] P. Cieśla, P. Kocot, P. Mytych, Z. Stasicka, J. Mol. Catal. A: Chem. 224 (2004) 17–33.
[251] J. Šima, J. Makáňová, Coord. Chem. Rev. 160 (1997) 161–189.
[252] H. Kawaguchi, A. Inagaki, Chemosphere 27 (1993) 2381–2387.
[253] P. Boule, M. Bolte, C. Richard, Environmental Photochemistry, Springer, 1999, pp. 181–215.
[254] E.P. Achterberg, T.W. Holland, A.R. Bowie, R.F.C. Mantoura, P.J. Worsfold, Anal. Chim. Acta 442 (2001) 1–14.
[255] W. Sunda, S. Huntsman, Mar. Chem. 84 (2003) 35–47.
[256] M. Schindler, M. Osborn, Biochemistry 18 (1979) 4425–4430.
[257] J.J. Pignatello, E. Oliveros, A. MacKay, Crit. Rev. Environ. Sci. Technol. 36 (2006) 1–84.
[258] X. Châtellier, D. Fortin, G.G. Leppard, F.G. Ferris, Eur. J. Mineral. 13 (2001) 705–714.
[259] X. Châtellier, M.M. West, J. Rose, D. Fortin, G.G. Leppard, F.G. Ferris, Geomicrobiol. J. 21 (2004) 99–112.
[260] J.F. Banfield, S.A. Welch, H. Zhang, T.T. Ebert, R.L. Penn, Science 289 (2000) 751–754.
[261] J.F. Banfield, H. Zhang, Rev. Mineral. Geochem. 44 (2001) 1–58.
[262] L. Emmenegger, R. Schönenberger, L. Sigg, B. Sulzberger, Limnol. Oceanogr. 46 (2001) 49–61.
[263] R.J. Hudson, F.M. Morel, F. Morel, Limnol. Oceanogr. 35 (1990) 1002–1020.
[264] R. Shwetharani, R. Geetha Balakrishna, J. Photochem. Photobiol. A: Chem. 295 (2014) 11–16.
[265] W. Köster, Res. Microbiol. 152 (2001) 291–301.

[266] H.G. Upritchard, J. Yang, P.J. Bremer, I.L. Lamont, A.J. McQuillan, Langmuir 23 (2007) 7189–7195.
[267] P.-C. Maness, S. Smolinski, D.M. Blake, Z. Huang, E.J. Wolfrum, W.A. Jacoby, Appl. Environ. Microbiol. 65 (1999) 4094–4098.
[268] C.L. Peacock, D.M. Sherman, Geochim. Cosmochim. Acta 68 (2004) 2623–2637.
[269] H. Wu, D. Jiang, P. Cai, X. Rong, Q. Huang, Colloids Surf. B: Biointerfaces 82 (2011) 147–151.
[270] B.M. Voelker, F.M.M. Morel, B. Sulzberger, Environ. Sci. Technol. 31 (1997) 1004–1011.
[271] Z. Zhang, C. Boxall, G. Kelsall, Colloids Surf. A: Physicochem. Eng. Aspects 73 (1993) 145–163.
[272] P. Mazellier, M. Bolte, J. Photochem. Photobiol. A: Chem. 132 (2000) 129–135.
[273] J. Xu, N. Sahai, C.M. Eggleston, M.A. Schoonen, Earth Planet. Sci. Lett. 363 (2013) 156–167.
[274] M. Brasca, S. Morandi, R. Lodi, A. Tamburini, J. Appl. Microbiol. 103 (2007) 1516–1524.
[275] F. Widdel, S. Schnell, S. Heising, A. Ehrenreich, B. Assmus, B. Schink, Nature 362 (1993) 834–836.
[276] Y. Xu, M.A. Schoonen, Am. Mineral. 85 (2000) 543–556.
[277] V. Buzmakov, A. Pshenichnikov, J. Colloid Interface Sci. 182 (1996) 63–70.
[278] R.C. Costa, M. Lelis, L. Oliveira, J. Fabris, J.D. Ardisson, R. Rios, C. Silva, R. Lago, J. Hazard. Mater. 129 (2006) 171–178.
[279] I.S. Pinto, P.H. Pacheco, J.V. Coelho, E. Lorençon, J.D. Ardisson, J.D. Fabris, P.P. de Souza, K.W. Krambrock, L.C. Oliveira, M.C. Pereira, Appl. Catal. B: Environ. 119 (2012) 175–182.
[280] S.C. Andrews, A.K. Robinson, F. Rodríguez-Quiñones, FEMS Microbiol. Rev. 27 (2003) 215–237.
[281] P.M. Borer, B. Sulzberger, P. Reichard, S.M. Kraemer, Mar. Chem. 93 (2005) 179–193.
[282] S.K. Han, T.-M. Hwang, Y. Yoon, J.-W. Kang, Chemosphere 84 (2011) 1095–1101.
[283] J. He, X. Tao, W. Ma, J. Zhao, Heterogeneous photo-fenton degradation of an Azo dye in aqueous H_2O_2/iron oxide dispersions at neutral pHs, Chem. Lett. 1 (2002) 86–87.
[284] K.M. Mostofa, C.-q. Liu, M.A. Mottaleb, G. Wan, H. Ogawa, D. Vione, T. Yoshioka, F. Wu, Photobiogeochemistry of Organic Matter, Springer, 2013, pp. 1–137.
[285] K. Mostofa, F. Wu, T. Yoshioka, H. Sakugawa, E. Tanoue, Natural Organic Matter and Its Significance in the Environment, Science Press, Beijing, 2009, pp. 3–66.
[286] R. Benner, J.D. Pakulski, Science 255 (1992) 1561.
[287] K. Isao, S. Hara, K. Terauchi, K. Kogure, Nature 345 (1990) 242–244.
[288] J.H. Sharp, Limnol. Oceanogr. 18 (1973) l–447.
[289] R.D. Vold, M.J. Vold, Colloid and Interface Chemistry, Addison-Wesley, 1983.
[290] M.L. Wells, 2002. Marine colloids and trace metals. Biogeochemistry of marine dissolved organic matter, pp. 367-404.
[291] K. Hayase, H. Tsubota, Geochim. Cosmochim. Acta 49 (1985) 159–163.
[292] X. Ma, N. Ali, Natural Organic Matter and its Significance in the Environment, Science Press, Beijing, 2009, pp. 66–89.
[293] F.J. Stevenson, in: G. Aiken, M. McKnight, R.L. Wershaw, P. MacCarthy (Eds.), Humic Substances in Soil, Sediment, and Water, Wiley, New York, 1985, pp. 13–52.
[294] A.M. Amado, J.B. Cotner, A.L. Suhett, F.d.A. Esteves, R.L. Bozelli, V.F. Farjalla, Aquat. Microb. Ecol. 49 (2007) 25–34.
[295] P.G. Coble, Mar. Chem. 51 (1996) 325–346.
[296] P.G. Coble, Chem. Rev. 107 (2007) 402–418.
[297] K. Mostofa, C. Liu, F. Wu, P. Fu, W. Ying, J. Yuan, Overview of key biogeochemical functions in lake ecosystem: impacts of organic matter pollution and global warming, in: Proceedings of 13th World Lake Conference, Wuhan, China, 2009, pp. 1–5.
[298] E. Parlanti, K. Wörz, L. Geoffroy, M. Lamotte, Org. Geochem. 31 (2000) 1765–1781.
[299] Y. Zhang, M.A. van Dijk, M. Liu, G. Zhu, B. Qin, Water Res. 43 (2009) 4685–4697.
[300] K.R. Arrigo, C.W. Brown, Impact of chromophoric dissolved organic matter on UV inhibition of primary productivity in the sea, Mar. Ecol. Progress Series 140 (1996) 207–216.
[301] N. Nelson, D. Siegel, A. Michaels, Deep Sea Res. I: Oceanogr. Res. Pap. 45 (1998) 931–957.
[302] N.B. Nelson, C.A. Carlson, D.K. Steinberg, Mar. Chem. 89 (2004) 273–287.
[303] C. Du, S. Shang, Q. Dong, C. Hu, J. Wu, Estuarine Coastal Shelf Sci. 88 (2010) 350–356.
[304] J.R. Helms, A. Stubbins, J.D. Ritchie, E.C. Minor, D.J. Kieber, K. Mopper, Limnol. Oceanogr. 53 (2008) 955–969.
[305] C.J. Hulatt, D.N. Thomas, D.G. Bowers, L. Norman, C. Zhang, Estuarine Coastal Shelf Sci. 84 (2009) 147–153.
[306] E. Rochelle-Newall, T. Fisher, Mar. Chem. 77 (2002) 23–41.
[307] S. Wada, M.N. Aoki, Y. Tsuchiya, T. Sato, H. Shinagawa, T. Hama, J. Exp. Mar. Biol. Ecol. 349 (2007) 344–358.
[308] Y. Dudal, R. Holgado, G. Maestri, E. Guillon, L. Dupont, Sci. Total Environ. 354 (2006) 286–291.
[309] A. Manciulea, A. Baker, J.R. Lead, Chemosphere 76 (2009) 1023–1027.
[310] J. Klinck, M. Dunbar, S. Brown, J. Nichols, A. Winter, C. Hughes, R.C. Playle, Aquat. Toxicol. 72 (2005) 161–175.
[311] M.L. Schwartz, P.J. Curtis, R.C. Playle, Environ. Toxicol. Chem. 23 (2004) 2889–2899.
[312] A.C. Stenson, A.G. Marshall, W.T. Cooper, Anal. Chem. 75 (2003) 1275–1284.
[313] A.T. Chow, J. Dai, W.H. Conner, D.R. Hitchcock, J.-J. Wang, Biogeochemistry 112 (2013) 571–587.
[314] D.M. White, D.S. Garland, J. Narr, C.R. Woolard, Water Res. 37 (2003) 939–947.
[315] H. Xie, O.C. Zafiriou, W.-J. Cai, R.G. Zepp, Y. Wang, Environ. Sci. Technol. 38 (2004) 4113–4119.
[316] E. Appiani, K. McNeill, Environ. Sci. Technol. 49 (2015) 3514–3522.
[317] M.L. Estapa, L.M. Mayer, Mar. Chem. 122 (2010) 138–147.
[318] J.R. Helms, D.A. Glinski, R.N. Mead, M.W. Southwell, G.B. Avery, R.J. Kieber, S.A. Skrabal, Org. Geochem. 73 (2014) 83–89.
[319] R.J. Kieber, R.F. Whitehead, S.A. Skrabal, Limnol. Oceanogr. 51 (2006) 2187–2195.
[320] L.M. Mayer, L.L. Schick, K. Skorko, E. Boss, Limnol. Oceanogr. 51 (2006) 1064–1071.
[321] M.W. Southwell, R.J. Kieber, R.N. Mead, G.B. Avery, S.A. Skrabal, Biogeochemistry 98 (2010) 115–126.
[322] S. Canonica, CHIMIA Int. J. Chem. 61 (2007) 641–644.
[323] G. McKay, F.L. Rosario-Ortiz, Environ. Sci. Technol. 49 (2015) 4147–4154.
[324] J. Buschmann, S. Canonica, L. Sigg, Environ. Sci. Technol. 39 (2005) 5335–5341.
[325] S. Canonica, M. Freiburghaus, Environ. Sci. Technol. 35 (2001) 690–695.
[326] K.M. Cawley, J.A. Hakala, Y.P. Chin, Limnol. Oceanogr.: Methods 7 (2009) 391–398.
[327] S. Halladja, A. Ter Halle, J.-P. Aguer, A. Boulkamh, C. Richard, Environ. Sci. Technol. 41 (2007) 6066–6073.
[328] L.E. Jacobs, L.K. Weavers, E.F. Houtz, Y.-P. Chin, Chemosphere 86 (2012) 124–129.
[329] P.G. Tratnyek, J. Hoigné, J. Photochem. Photobiol. A: Chem. 84 (1994) 153–160.
[330] D. Vione, M. Minella, V. Maurino, C. Minero, Chem. Eur. J. 20 (2014) 10590–10606.
[331] W.J. Cooper, R.G. Zika, Science (Washington) 220 (1983) 711–712.
[332] W.J. Cooper, R.G. Zika, R.G. Petasne, J.M. Plane, Environ. Sci. Technol. 22 (1988) 1156–1160.
[333] W.M. Draper, D.G. Crosby, Arch. Environ. Contam. Toxicol. 12 (1983) 121–126.
[334] N. Scully, D. McQueen, D. Lean, Limnol. Oceanogr. 41 (1996) 540–548.
[335] D.T. Scott, R.L. Runkel, D.M. McKnight, B.M. Voelker, B.A. Kimball, E.R. Carraway, Water Resour. Res. 39 (2003).
[336] S.S. Andrews, S. Caron, O.C. Zafiriou, Limnol. Oceanogr. 45 (2000) 267–277.
[337] J.H. Jerome, R.P. Bukata, J. Great Lakes Res. 24 (1998) 929–935.
[338] C.A. Moore, C.T. Farmer, R.G. Zika, J. Geophys. Res. 98 (1993) 2289–2298.
[339] R.J. Sikorski, R.G. Zika, J. Geophys. Res. 98 (1993) 2315–2328.
[340] B.H. Yocis, D.J. Kieber, K. Mopper, Deep Sea Res. I: Oceanogr. Res. Pap. 47 (2000) 1077–1099.
[341] E.M. White, P.P. Vaughan, R.G. Zepp, Aquat. Sci. 65 (2003) 402–414.
[342] D.M. McKnight, B.A. Kimball, R.L. Runkel, Hydrol. Process. 15 (2001) 1979–1992.
[343] R.K. Skogerboe, S.A. Wilson, Anal. Chem. 53 (1981) 228–232.
[344] M. Sanly, K.C. Lim, R. Amal, R. Fabris, C. Chow, M. Drikas, Sep. Sci. Technol. 42 (2007) 1391–1404.
[345] B.A. Southworth, B.M. Voelker, Environ. Sci. Technol. 37 (2003) 1130–1136.
[346] A. Moncayo-Lasso, A.G. Rincon, C. Pulgarin, N. Benitez, J. Photochem. Photobiol. A: Chem. 229 (2012) 46–52.
[347] N.V. Blough, R.G. Zepp, Active Oxygen in Chemistry, Springer, 1995, pp. 280–333.
[348] H. Gao, R.G. Zepp, Environ. Sci. Technol. 32 (1998) 2940–2946.
[349] H. Tamura, K. Goto, M. Nagayama, Corros. Sci. 16 (1976) 197–207.
[350] C. Siffert, B. Sulzberger, Langmuir 7 (1991) 1627–1634.
[351] A. Paul, S. Hackbarth, R.D. Vogt, B. Röder, B.K. Burnison, C.E.W. Steinberg, Photochem. Photobiol. Sci. 3 (2004) 273–280.
[352] S.L.H. Sandvik, P. Bilski, J.D. Pakulski, C.F. Chignell, R.B. Coffin, Mar. Chem. 69 (2000) 139–152.
[353] D.J. Kieber, N.V. Blough, Free Radical Res. 10 (1990) 109–117.
[354] M.A. Moran, R.G. Zepp, Limnol. Oceanogr. 42 (1997) 1307–1316.
[355] R.L. Valentine, R.G. Zepp, Environ. Sci. Technol. 27 (1993) 409–412.
[356] R. Del Vecchio, N.V. Blough, Mar. Chem. 78 (2002) 231–253.
[357] R.G. Zepp, Solar UVR and aquatic carbon, nitrogen, sulfur and metals cycles. UV effects in aquatic organisms and ecosystems, Royal Soc. Chem. (2003) 137–184.
[358] A. Georgi, A. Schierz, U. Trommler, C.P. Horwitz, T.J. Collins, F.D. Kopinke, Appl. Catal. B: Environ. 72 (2007) 26–36.
[359] S.G. Huling, R.G. Arnold, R.A. Sierka, M.R. Miller, Water Res. 35 (2001) 1687–1694.
[360] J. Kochany, E. Lipczynska-Kochany, Environ. Technol. 28 (2007) 1007–1013.
[361] C. Kuei-Jyum Yeh, Y.A. Kao, C.P. Cheng, Chemosphere 46 (2002) 67–73.
[362] E. Lipczynska-Kochany, J. Kochany, Chemosphere 73 (2008) 745–750.
[363] C.A. Murray, S.A. Parsons, Chemosphere 54 (2004) 1017–1023.
[364] D. Spuhler, J.A. Rengifo-Herrera, C. Pulgarin, Appl. Catal. B: Environ. 96 (2010) 126–141.
[365] A.W. Vermilyea, B.M. Voelker, Environ. Sci. Technol. 43 (2009) 6927–6933.
[366] D. Vione, G. Falletti, V. Maurino, C. Minero, E. Pelizzetti, M. Malandrino, R. Ajassa, R.I. Olariu, C. Arsene, Environ. Sci. Technol. 40 (2006) 3775–3781.

[367] G.K.B. Lopes, H.M. Schulman, M. Hermes-Lima, Biochim. Biophys. Acta Gen. Subj. 1472 (1999) 142–152.
[368] C. Tixier, H.P. Singer, S. Canonica, S.R. Müller, Environ. Sci. Technol. 36 (2002) 3482–3489.
[369] B.W. Bogan, V. Trbovic, J. Hazard. Mater. 100 (2003) 285–300.
[370] M.E. Lindsey, M.A. Tarr, Environ. Sci. Technol. 34 (2000) 444–449.
[371] M.E. Lindsey, M.A. Tarr, Chemosphere 41 (2000) 409–417.
[372] L.L. Bissey, J.L. Smith, R.J. Watts, Water Res. 40 (2006) 2477–2484.
[373] Z.M. Li, P.J. Shea, S.D. Comfort, Chemosphere 36 (1998) 1849–1865.
[374] B.W. Tyre, R.J. Watts, G.C. Miller, J. Environ. Qual. 20 (1991) 832–838.
[375] T.W. Ng, A.T. Chow, P.K. Wong, J. Photochem. Photobiol. A: Chem. 290 (2014) 116–124.
[376] J.J. Guerard, P.L. Miller, T.D. Trouts, Y.P. Chin, Aquat. Sci. 71 (2009) 160–169.
[377] J. Wenk, U. von Gunten, S. Canonica, Environ. Sci. Technol. 45 (2011) 1334–1340.
[378] M.F. Budyka, M.V. Alfimov, Russ. Chem. Rev. 64 (1995) 705–717.
[379] M. Roca, J. Zahardis, J. Bone, M. El-Maazawi, V.H. Grassian, J. Phys. Chem. A 112 (2008) 13275–13281.
[380] R.G. Zepp, J. Hoigné, H. Bader, Environ. Sci. Technol. 21 (1987) 443–450.
[381] P. Warneck, C. Wurzinger, J. Phys. Chem. 92 (1988) 6278–6283.
[382] K. Wakabayashi, M. Nagao, T. Sugimura, Cancer Surv. 8 (1988) 385–399.
[383] H.Y. Chen, O. Zahraa, M. Bouchy, J. Photochem. Photobiol. A: Chem. 108 (1997) 37–44.
[384] J.E. Grebel, J.J. Pignatello, W.A. Mitch, Environ. Sci. Technol. 44 (2010) 6822–6828.
[385] C.-H. Liao, S.-F. Kang, F.-A. Wu, Chemosphere 44 (2001) 1193–1200.
[386] J. Cadet, T. Douki, J.-L. Ravanat, P. Di Mascio, Photochem. Photobiol. Sci. 8 (2009) 903–911.